

Responsive deep brain stimulation guided by ventral striatal electrophysiology of obsession durably ameliorates compulsion

Highlights

- We reported a first-in-human application of responsive deep brain stimulation for OCD
- The area-based feature triggered closed-loop stimulation to ameliorate OCD symptoms
- We identified an association between NAc-VeP low-frequency oscillatory power and OCD
- We provided a concept for a personalized, physiologically guided DBS strategy for OCD

Authors

Young-Hoon Nho, Camarin E. Rolle, Uros Topalovic, ..., Nanthia Suthana, Daniel A.N. Barbosa, Casey H. Halpern

Correspondence

dbarbosa@penntmedicine.upenn.edu (D.A.N.B.),
casey.halpern@penntmedicine.upenn.edu (C.H.H.)

In brief

We report on a first-in-human application of responsive deep brain stimulation (rDBS) of the ventral striatum for treatment-refractory OCD. rDBS detected the time-domain area-based feature from invasive electroencephalography low-frequency oscillatory power fluctuations that triggered bursts of stimulation to ameliorate OCD symptoms in a closed-loop fashion.



Case Study

Responsive deep brain stimulation guided by ventral striatal electrophysiology of obsession durably ameliorates compulsion

Young-Hoon Nho,^{1,9} Camarin E. Rolle,^{1,9} Uros Topalovic,² Rajat S. Shivacharan,³ Tricia N. Cunningham,³ Sonja Hiller,² Daniel Batista,² Austin Feng,³ Flint M. Espil,⁴ Ian H. Kratter,⁴ Mahendra T. Bhati,^{3,4} Marissa Kellogg,⁵ Ahmed M. Raslan,⁶ Nolan R. Williams,⁴ John Garnett,³ Bijan Pesaran,¹ Desmond J. Oathes,⁷ Nanthia Suthana,² Daniel A.N. Barbosa,^{1,*} and Casey H. Halpern^{1,8,10,*}

¹Department of Neurosurgery, University of Pennsylvania, Philadelphia, PA, USA

²Department of Psychiatry and Biobehavioral Sciences, Jane and Terry Semel Institute for Neuroscience and Human Behavior, University of California, Los Angeles, Los Angeles, CA, USA

³Department of Neurosurgery, Stanford University School of Medicine, Stanford, CA, USA

⁴Department of Psychiatry and Behavioral Sciences, Stanford University School of Medicine, Stanford, CA, USA

⁵Oregon Health and Science University Comprehensive Epilepsy Center, Portland, OR, USA

⁶Department of Neurological Surgery, Oregon Health & Science University, Portland, OR, USA

⁷Department of Psychiatry, Center for Neuromodulation in Depression and Stress, Brain Science, Translation, Innovation, and Modulation Center, University of Pennsylvania, Philadelphia, PA, USA

⁸Department of Surgery, Corporal Michael J. Crescenz Veterans Affairs Medical Center, Philadelphia, PA, USA

⁹These authors contributed equally

¹⁰Lead contact

*Correspondence: dbarbosa@pennmedicine.upenn.edu (D.A.N.B.), casey.halpern@pennmedicine.upenn.edu (C.H.H.)

<https://doi.org/10.1016/j.neuron.2023.09.034>

SUMMARY

Treatment-resistant obsessive-compulsive disorder (OCD) occurs in approximately one-third of OCD patients. Obsessions may fluctuate over time but often occur or worsen in the presence of internal (emotional state and thoughts) and external (visual and tactile) triggering stimuli. Obsessive thoughts and related compulsive urges fluctuate (are episodic) and so may respond well to a time-locked brain stimulation strategy sensitive and responsive to these symptom fluctuations. Early evidence suggests that neural activity can be captured from ventral striatal regions implicated in OCD to guide such a closed-loop approach. Here, we report on a first-in-human application of responsive deep brain stimulation (rDBS) of the ventral striatum for a treatment-refractory OCD individual who also had comorbid epilepsy. Self-reported obsessive symptoms and provoked OCD-related distress correlated with ventral striatal electrophysiology. rDBS detected the time-domain area-based feature from invasive electroencephalography low-frequency oscillatory power fluctuations that triggered bursts of stimulation to ameliorate OCD symptoms in a closed-loop fashion. rDBS provided rapid, robust, and durable improvement in obsessions and compulsions. These results provide proof of concept for a personalized, physiologically guided DBS strategy for OCD.

INTRODUCTION

Obsessive-compulsive disorder (OCD) is characterized by recurrent, distressing thoughts (obsessions) that may be temporarily alleviated by repetitive, ritualized behaviors (compulsions), both of which disrupt activities of daily life.^{1,2} OCD is a chronic psychiatric disorder that affects approximately 2.2 million adults across all demographics. With more than 200,000 new cases in the US annually, OCD ranks among the most common psychiatric disorders.³ Several treatments exist for OCD, including psychological (e.g., exposure and response prevention⁴), pharmacological (e.g., serotonergic antidepressants), and repetitive transcranial magnetic stimulation.^{5,6} Despite the availability of

a variety of treatments, approximately one in three patients who seek treatment for OCD can be classified as treatment resistant (trOCD) based on the lack of clinically significant response.^{7,8}

Deep brain stimulation (DBS) targeting ventral striatal regions is a US Food and Drug Administration-approved therapy for trOCD under a humanitarian device exemption. Although DBS approximately achieves a 50% response rate, patient outcomes are markedly heterogeneous.⁹ Failure to achieve consistent outcomes is multifactorial, but one critical limitation may be that DBS (and neuroablation) does not specifically respond to the corollary neural activity of fluctuating obsessions or the subsequent escalating urges to compulsive to relieve them. Utilizing



symptom-related electrophysiology to guide a responsive stimulation bout may provide more optimal treatment and is supported by positive findings in preclinical and clinical studies of compulsive behavior.¹⁰

Responsive deep brain stimulation (rDBS) provides a means of delivering stimulation episodically and only in response to symptom-relevant physiology. Such responsive intracranial stimulation has prior validation in the cortex for partial-onset epilepsy, as well as depression,^{11,12} using the responsive neurostimulation (RNS) system (NeuroPace),^{13–15} and unlike conventional DBS that is continuous, this strategy provides brief bouts of acute stimulation in response to detections of a pre-specified electrophysiologic signal. This system incorporates patient-initiated annotations of the electrophysiologic recordings to time-lock them to relevant behaviors or symptoms experienced by the patient.¹⁶ Conventional DBS has previously been utilized in OCD for biomarker identification in the STN.^{17–19} However, to date, the symptom-related electrophysiology of the nucleus accumbens, a known region implicated in OCD, has never been investigated in an ambulatory setting.

Here, we report the first case of rDBS targeted to the ventral striatum, involving the nucleus accumbens and ventral pallidum (NAc-VeP) regions, specifically to treat trOCD in a patient with comorbid epilepsy. Importantly, we set forward a series of analytic steps taken to characterize and validate the symptom-related signal used to trigger rDBS delivery in this patient. We attempted to identify a NAc-VeP electrophysiologic signal (the differential signal recorded between two invasive electroencephalography (iEEG) electrodes—one in the NAc and one in the VeP) associated with OCD symptoms occurring in naturalistic, ambulatory settings and as provoked during in-lab behavioral tasks. Specifically, data were acquired from three types of tasks—(1) ambulatory: data acquired from the patient at home both while asymptomatic and time-locked to moments of obsessions; (2) naturalistic provocation task: data acquired in lab, time-locked to the patient's overt interaction both with neutral items (items that do not provoke OCD-related distress) and obsession-related items (items that do provoke OCD-related distress); and (3) virtual reality (VR) provocation task: data acquired in lab, time-locked to the patient's virtual interaction with both neutral and obsessive items. Primary analyses focused on the time-domain area-based feature (area under the curve [AUC] of recordings) and spectral power so that the findings could be more easily translated to a detector triggering rDBS. We then implemented rDBS triggered by NAc-VeP electrophysiology identified from ambulatory and in-lab tasks and report here the clinical results suggesting the potential efficacy of this treatment for trOCD. Finally, we investigated signals driving rDBS detections as a validation of the spectral properties underlying AUC fluctuations.

RESULTS

Two leads were implanted 7 months prior to OCD stimulation, and the patient received stimulation to treat epilepsy following surgery. As derived from this patient's epilepsy surgical case conference, there was consensus that a neuromodulatory strategy was her safest option, having had a prior anterior temporal

lobectomy. Seizure monitoring revealed rapid spread to the insula, and this was corroborated by prior peri-insular activation on single-photon emission computed tomography. Therefore, consensus was to offer rDBS with depth leads placed in right superior temporal lobe/Heschl's gyrus and the right peri-insular area (depths were preferred over strips by the surgical team for safety). Thus, an off-label electrode utilized for rDBS in this patient with epilepsy and comorbid severe OCD followed a novel trajectory (see [STAR Methods](#)), traversing the peri-insula region and implicating two critical, deep adjacent nodes within the right ventral striatum, with one electrode contact in the posterior border of the VeP and the most distal electrode contact in the ventral anterior border of the NAc ([Figures 1A and S1](#)). The patient described significant impairment of her daily functioning due to her OCD symptoms (e.g., doors and windows checking for safety or being afraid of eating with other people), had undergone a number of psychological and pharmacological treatments for OCD with limited to no benefit, and was taking stable doses of sertraline and several anticonvulsant medications with limited benefit.

As true detections (resulting in stimulation) are only captured within the long-episode iEEG data, we will use the term “peaks” to refer to above-threshold peaks identified via peak analyses within our manuscript, “detections” to more specifically refer to true detections captured in the long-episode iEEG data, and “detection count” to refer to the daily number of detections, including single- and long-episode detections. Our analyses first quantified the OCD-related signal by analyzing NAc-VeP iEEG data acquired during OCD-related distress in three experimental conditions: (1) ambulatory, patient-initiated magnet-swipe storage of data during moments of obsessive thoughts; (2) lab-based, naturalistic provocation of OCD-related distress (naturalistic provocation task); and (3) lab-based, VR provocation of OCD-related distress (VR provocation task). The rDBS system is able to trigger stimulation based on elevations in AUC. Therefore, AUC trends were extracted from time-locked OCD distress trials, quantified, and then compared with control periods for each assessment ([Video S1](#)). We then extracted peaks in AUC to determine the number and amplitude of AUC peaks. Finally, we extracted frequency power specific to the AUC peaks to identify any frequency-specific contributions to the AUC estimates. The above analyses were also applied to OCD-detection snapshots of data that triggered bouts of stimulation.

Nac-VeP electrophysiology

An off-label electrode utilized for rDBS in a patient with comorbid OCD and epilepsy followed a novel trajectory (see [STAR Methods](#)), implicating two critical, adjacent nodes within the right ventral striatum, with one electrode contact in the posterior border of the VeP and the most distal electrode contact in the ventral anterior border of the NAc ([Figure 1A](#)). The goal of the analyses hereby described was to identify electrophysiologic signals in this region that correlated with moments of obsession and use these signals to trigger rDBS via an AUC detection algorithm (see [STAR Methods](#) for more details). We performed these analyses on samples of iEEG recorded during episodes associated with obsessions (and control periods) and their resulting compulsions. We then extracted spectral information from this

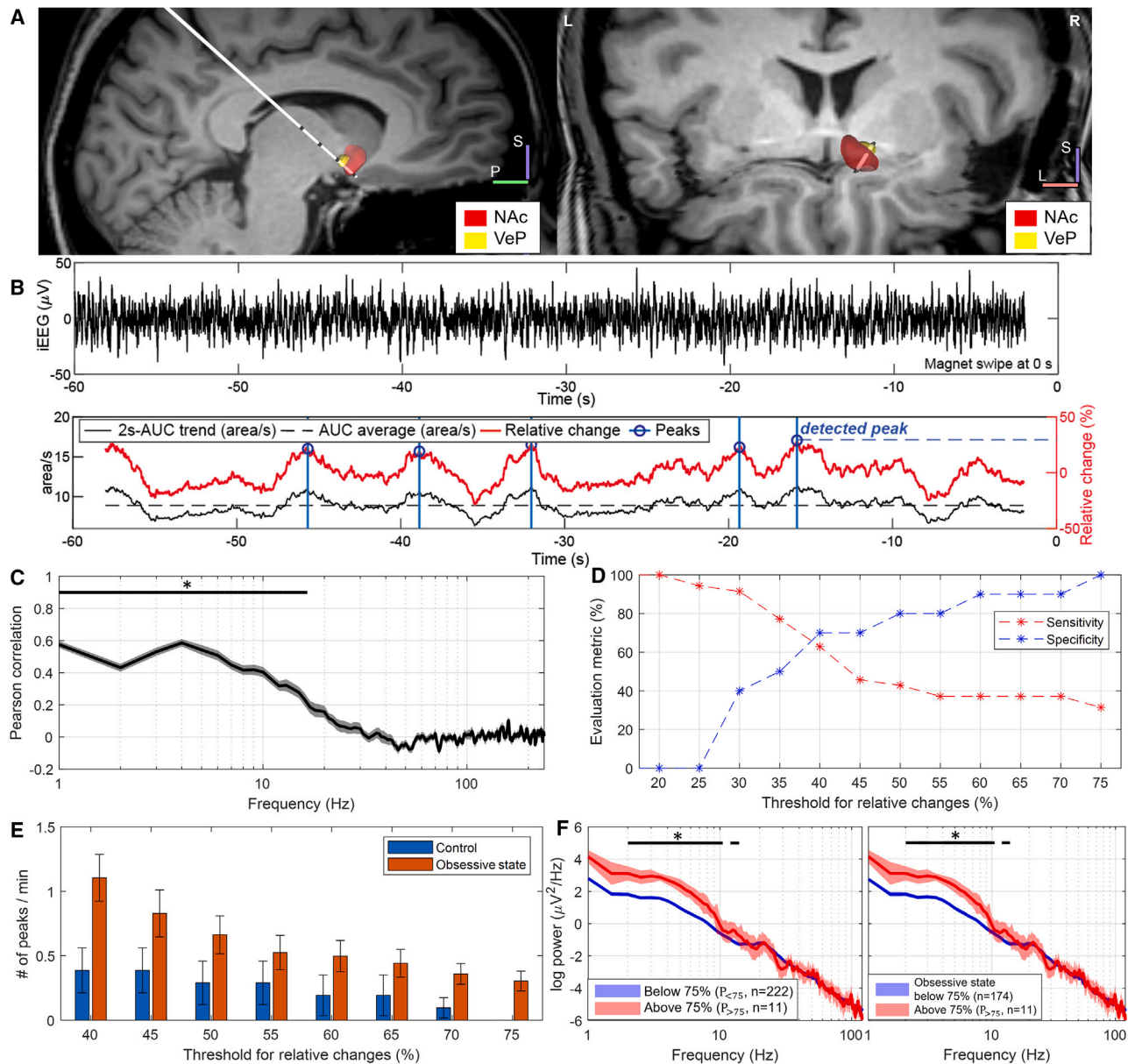


Figure 1. NAc-VeP electrophysiology derived from ambulatory task

(A) Postoperative computed tomography (CT) and preoperative magnetic resonance imaging (MRI) were co-registered to localize the rDBS electrode contacts: one electrode contact was located in the posterior border of the right VeP, and the other electrode contact was in the ventral anterior border of the right NAc. This lead was off-label in an attempt to treat OCD in a patient with comorbid partial-onset epilepsy. Another lead targeting the right temporal lobe is not depicted in this figure but delivered stimulation when a seizure was detected.

(B) Top: iEEG trace from bipolar re-referencing between NAc and VeP. Bottom: 2 s-AUC short-term trend (black line) was extracted from iEEG, and relative change (red line) of AUC from the average (black dotted line) and peaks (blue circle). The peaks were detected and extracted using the MATLAB function to find local maxima (blue circle). The relative changes at these peaks were quantified in our analyses. The blue vertical lines are instances when the threshold detection settings, % change in AUC, detected a peak in the AUC, i.e., when responsive stimulation would be triggered.

(C) Pearson correlation between 2 s-AUC short-term trend across the spectral power. Low-frequency ranges had a significant correlation with 2 s-AUC in 1/f corrected power (<15 Hz) (one-sample two-sided sign test, and FDR-adjusted * $p < 0.001$).

(D) Sensitivity and specificity for various threshold settings from ambulatory task. We can examine how accurate the rDBS is with the threshold changes.

(E) The number of peaks when relative changes exceed threshold derived from ambulatory task (mean \pm SEM). Only the obsessive state iEEG snapshots had peaks over the 75% increase in AUC.

(F) Comparison of spectral power at AUC peaks with amplitude below vs. exceeding 75% of the long-term trend in both obsessive state and control (left), and below vs. exceeding 75% in the obsessive states (right). Peaks exceeding the 75% threshold (only observed in obsessive iEEG snapshots) had greater low-frequency power (<15 Hz) compared with peaks below the 75% threshold observed in both obsessive and control iEEG snapshots (FDR-adjusted * $p < 0.001$, one-sided Student's t test).

signal to better understand the frequency contributions to the AUC. We applied the same analyses to lab-based provocation procedures to examine the signal in a more controlled setting. Finally, we confirmed the relevance of this signal to rDBS clinical outcomes by applying these AUC and spectral analyses to the iEEG signal triggering rDBS.

Tasks

Obsession-related distress, captured both in naturalistic ambulatory settings as well as in experimental task-based provocations, was associated with peaks in AUC. The magnitude of these peaks in AUC correlated with the low-frequency power.

Ambulatory task

The ambulatory analyses used data acquired from the patient at home, both while asymptomatic and time-locked to moments of obsession. The first analyses focused on characterizing ambulatory data before enabling the rDBS strategy. The ambulatory iEEG snapshots were patient-initiated by a magnet swipe over the neurostimulator, and the patient was instructed to initiate such recordings during two states: (1) “obsessive” iEEG snapshots ($n = 35$): when the patient experienced obsessive thoughts around her safety prior to beginning her compulsion (e.g., checking doors, windows, and appliances), and (2) “control” iEEG snapshots ($n = 10$): when the patient was asymptomatic.

Our primary analysis extracted the AUC of the iEEG signal, quantified as the area between the raw iEEG signal and “0” on the x axis (which reflects amplitude of the raw signal). This metric was extracted because the rDBS detection algorithm relies on above-threshold elevations in AUC (Figure 1B). Specifically, the intracalvarial neurostimulator calculates the relative change between a moving short-term trend (e.g., 2-s window) AUC average compared with a moving long-term trend (e.g., 2-min window) AUC average and then delivers stimulation when the short-term trend exceeds the long-term trend by designated threshold criteria. To characterize spectral contributions driving fluctuations in the AUC, we analyzed the correlations with spectral power across the available spectrum (1–120 Hz). We found that the power in the low-frequency signal (<15 Hz for 1/f corrected power) was the most highly correlated with AUC, whereas higher frequencies were weakly correlated with AUC, converging to a correlation coefficient of zero at more than 15 Hz with false discovery rate (FDR) adjusted $*p < 0.001$; sign test (Figure 1C).

We then extracted control and obsessive iEEG snapshots (3 min in duration) and simulated detection parameters to isolate properties of the iEEG contributing to the detections. First, at a detection threshold of 75%, we found obsessions were detected at 31.4% sensitivity (the proportion of detected obsessive states out of all obsessive states) and 100% specificity (the proportion of detected controls out of all controls) (Figure 1D). As the rDBS detections were triggered by the relative change in AUC (short-term vs. long-term trend), we then extracted the local maxima (peaks) in the relative change, grouping them into two classes—those above the 75% ($P_{>75}$) vs. below the 75% ($P_{<75}$) relative change threshold. $P_{>75}$ were only found within obsessive, and not control, snapshots (Figure 1E) (mean \pm SEM). Finally, we extracted spectral power at each peak. The power in $P_{>75}$ (only observed in obsessive snapshots) had a significant eleva-

tion in low-frequency power (<15 Hz) compared with $P_{<75}$ (FDR-adjusted $*p < 0.001$, Student’s t test) (Figure 1F). Frequencies above 15 Hz did not significantly differ in power between $P_{>75}$ and $P_{<75}$ (FDR-adjusted $*p < 0.001$, Student’s t test).

In summary, our analyses of the ambulatory snapshots of iEEG data that corresponded to moments of obsession validated that (1) low-frequency signal <15 Hz was the strongest spectral contributor to AUC estimates driving rDBS detections in this patient, (2) peaks in relative change exceeding the 75% relative change threshold (modeled after therapeutic detector settings) were only found during obsessive snapshots, and (3) low-frequency power (<15 Hz) was significantly more prominent in $P_{>75}$ compared with $P_{<75}$.

Provocation tasks

To validate our ambulatory results with more experimentally controlled tasks, we applied our analyses to both naturalistic and VR provocation tasks. Examples of naturalistic and VR provocation tasks are visualized in Figure 2A. Both provocation tasks quantified iEEG during the patient’s interaction with (1) neutral items (items that did not provoke OCD-related distress) and (2) obsessive items (items that did provoke OCD-related distress). Obsessive items are items that, when encountered by the patient, provoke obsessions and triggered an urge to compulsive. Subjective unit of distress (SUDS) ratings were recorded, which confirmed an increase in distress only with items known to provoke the patient’s obsessions (see STAR Methods for SUDS ratings).

Similar to the ambulatory analyses, we extracted “neutral” and obsessive trials and simulated detection parameters to isolate properties of the iEEG contributing to the detections. Our first analyses aimed to identify the detection threshold (AUC short-term/long-term trend ratio) that would maximize specificity for obsessive trials. Maximal specificity—no false positive detections of control trials—was achieved with a detection threshold of 35% for the naturalistic provocation task. At 35% detection threshold, sensitivity to obsessive trials was 28.6% (Figure 2B, top). In other words, only obsessive trials had $P_{>35}$, but only 28.6% of the obsessive trials had a $P_{>35}$, resulting in a 0% false positive rate but a 71.4% false negative rate. Maximal specificity was achieved with a detection threshold of 50% for the VR provocation task. At a 50% detection threshold, sensitivity to obsessive trials was 27.27% (Figure 2B, bottom). Again, in other words, $P_{>50}$ was only present in obsessive snapshots, but only 27.27% of those obsessive trials contained $P_{>50}$.

As opposed to the naturalistic provocation task, the VR provocation task included items with distinct levels of reported distress. Therefore, we analyzed peaks as they related to distinct ratings to account for the impact of different levels of elicited distress on the observed peaks. The VR provocation task was rated on a -3 (very distressful) to $+3$ (very comfortable) Likert scale. The patient only reported a distress level of -3 ($n = 3$) and -2 ($n = 8$). This analysis found that $P_{>65}$ was only observed during high distress levels (-3) compared with low distress (i.e., -2) (Figure S2A). For the receiver operator characteristic (ROC) curve that plots the true positive rate vs. the false positive rate, the area under the ROC curve was 0.89 for high distress ratings (-3) but just 0.62 for low distress ratings (-2), indicating that the diagnostic accuracy (area under the ROC curve) was related

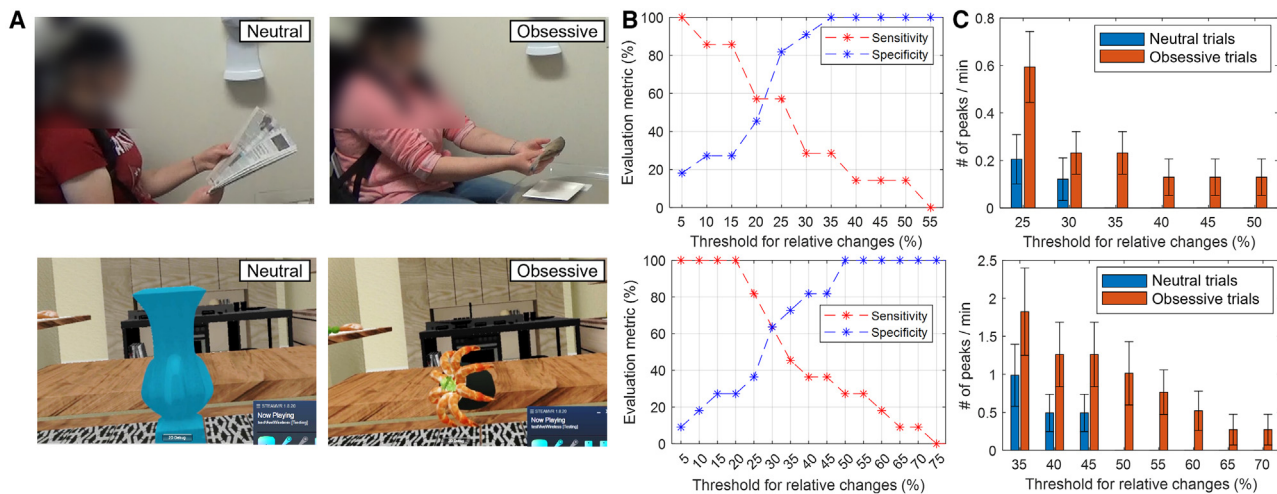


Figure 2. NAc-VeP electrophysiology derived from laboratory-based provocation of obsession

(A) Top row: naturalistic provocation task; bottom row: items in VR provocation task.

(B) Sensitivity and specificity for various threshold settings from the naturalistic provocation task (top) and the VR provocation task (bottom).

(C) The number of peaks when relative changes exceed the designated threshold (mean \pm SEM) from the naturalistic provocation task (top) and the VR provocation task (bottom). Only obsessive trials were observed with higher thresholds.

to the level of distress associated with the obsession-provoking trials (Figures S2B and S2C).

We then sought to identify any spectral power differences between neutral and obsessive trials. The greatest power difference during interaction with obsessive compared with neutral items was found for the low-frequency range visualized with red (Figure 3A), ~ 1 s following the beginning of the stimulus presentation for both provocation tasks. Baseline normalized band-averaged spectral power (1–4 Hz frequencies; delta) was significantly elevated during interaction with obsessive items compared with neutral items (Figure 3B, cluster-based permutation test, $*p < 0.05$). We did not observe any significant changes in the other frequency bands. The absolute power (not normalized to a baseline time period) was also elevated (1–4 Hz for naturalistic, 1–2 Hz for VR) during interactions with obsessive items (Figure 3C, one-sided Student's *t* test, FDR-adjusted $*p < 0.01$).

rDBS therapeutic outcomes Obsession/compulsion severity

The patient's baseline Yale-Brown Obsessive-Compulsive Scale (Y-BOCS)^{20,21} score was 32 (obsessions, 17; compulsions, 15) and decreased to 20 (obsessions, 8; compulsions, 12) 24 h post-Nac-VeP-rDBS activation, a 37.5% reduction. Serial self-reported Y-BOCS (Y-BOCS-SR²²) were completed over the next 2 years 22 weeks, and a progressive and durable decrease was noted (biweekly, first month, intermittently afterward) (Figure 4A). The patient's Y-BOCS score at 1 year 18 weeks post-Nac-VeP-rDBS activation (obsessions, 8; compulsions, 8) provided a percent change from baseline of 50.0%, which exceeds the $>35\%$ reduction threshold typically used to define treatment response in OCD.^{23,24} The maximum Y-BOCS-SR score improvement occurred at 1 year 45 weeks and then again at 2 years 16 weeks, at which time the percent Y-BOCS-SR change from 24 h post-Nac-VeP-rDBS activation was 50.0% (from 18 to 9).

As part of an exploratory analysis, we correlated the Y-BOCS-SR scores (capturing self-reported symptoms over last 7 days) with two ambulatory metrics (averaged across the 7 days preceding each Y-BOCS-SR report): (1) detection count (number of daily detections, $>500/\text{day}$; Figures S3A and S3B) and (2) low-frequency power (extracted from stored long-episode iEEG snapshots, on average 3/day; Figures S3C and S3D). These analyses found that although detection count did not correlate with Y-BOCS-SR ($p = 0.749$), low-frequency power (1–15 Hz) correlated with Y-BOCS-SR ($p = 0.0017$), holding for both the obsession subscore ($p = 0.0019$) and compulsion subscore ($p = 0.0005$). Although these exploratory analyses have limitations that impact interpretability of these results (detailed in the discussion section), these findings do suggest that low-frequency power may scale with symptom severity, supporting our main findings showing the relevance of low-frequency power to OCD.

Subjective self-report

Prior to Nac-VeP-rDBS activation, the patient was living with her parents. She suffered from safety- and contamination-related obsessions, which could only be relieved by compulsive safety checking and handwashing. She referred to her OCD symptoms as more debilitating than her epilepsy, despite having had life-threatening seizures (though these had stabilized prior to initiating this intervention for her OCD and remained stable throughout this treatment). She reported spending 3 h/day performing her compulsions and had documented multiple unsuccessful therapeutic trials of medication and cognitive-behavioral therapy. At the 24-week follow-up, the patient reported that she was no longer experiencing some of her obsessions and, consequently, was not feeling the urge to engage in compulsive behaviors, including several of her safety-related checking routines. The therapeutic effect has remained durable over the past year. At her most recent follow-up (2 years and 22 weeks after

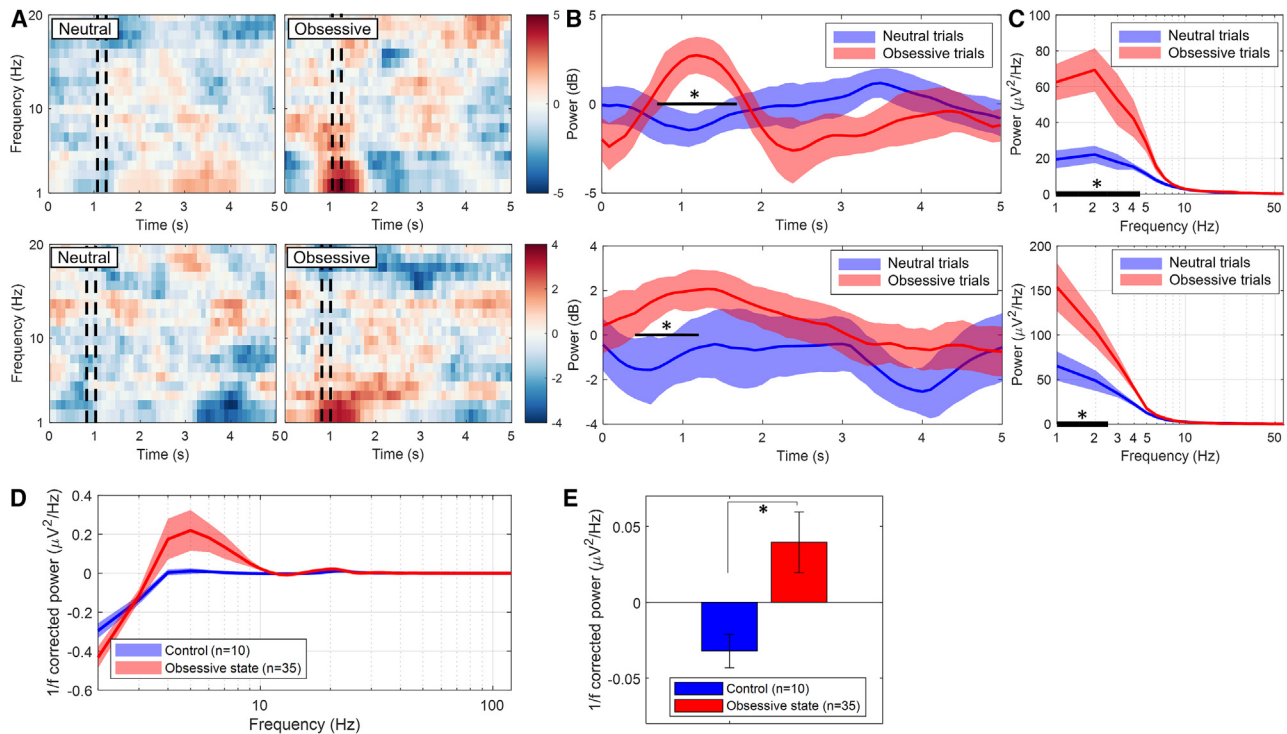


Figure 3. In-lab provocation tasks and symptom-locked ambulatory electrophysiologic data all found low-frequency oscillations to be elevated during obsessive states

(A) Spectrograms after touch interaction ($t = 0$). Top row: naturalistic provocation task; bottom row: VR provocation task.
 (B) Baseline normalized delta-frequency range (1–4 Hz) power in each condition (top: naturalistic; bottom: VR provocation tasks). There were significant power changes after touch interaction ($*p < 0.05$).
 (C) Absolute powers in the dash lines of (A). 1–4 Hz (naturalistic) and 1–2 Hz (VR) absolute power of interaction with obsessive food are significantly higher than interaction with neutral items (FDR-adjusted $*p < 0.01$).
 (D) We quantified the power from 1–120 Hz for ambulatory (magnet-swipe stored) snapshots of data (60 to 2 s preceding the magnet-swipe), comparing self-reported control and obsessive states. We did not find a significant difference in power between these two conditions for the ambulatory stored data at any specific frequency (FDR-adjusted $p \geq 0.6553$).
 (E) As 2 s-AUC was found to specifically correlate with power < 15 Hz, we averaged ambulatory power from 1–15 Hz and compared between conditions. Average ambulatory power from 1–15 Hz in obsessive state was significantly higher than the power of control ($*p < 0.05$, one-sided Student's *t* test).

surgery), the patient reported that she has had a life-changing improvement in her OCD symptoms. She estimated that she now spends 30 min/day performing compulsions (down from more than 8 h/day) and is able to do things that she had previously deemed impossible, such as being able to sit next to someone eating something that previously would have triggered her contamination obsessions (e.g., seafood) and to leave the house without engaging in much of her previous checking routine, such that she is no longer late for work. She has also resumed living independently for the first time in many years.

Detections

The rDBS therapy was delivered based on AUC detection (a charge density of $7.1 \mu\text{C}/\text{cm}^2$, a current of 7.0 mA, a frequency of 125 Hz, a pulse width per phase of 80 μs , and a burst duration of 1,000 ms), and we investigated the relative changes in power underlying AUC detections for 2 years 4 months after stimulation was enabled (Figure 4B). Note that Figures 4B and 4C were based on long-episode detections data that resulted from more than five consecutive detections within a 20-s interval (see STAR Methods). Stimulation was delivered at two different

thresholds (75% from 2019 to 2020, and 87.5% from 2021 to now). After stimulation was enabled, relative power preceding AUC detections decreased for the first 5 months (November 2019 to March 2020), most prominently in the delta (1–4 Hz), theta (5–8 Hz), and alpha (9–12 Hz) bands. After 5 months, the detection power stabilized. Following stabilization of detection-related power, which was most prominent after adjusting the detection threshold to 87.5% in 2021, detection-locked power was elevated in the 1–4 Hz delta-frequency range (Figure 4B). We found the power above 11 Hz was not significantly different compared with zero. In other words, the low-frequency (< 11 Hz) power was significantly greater than zero in both detection thresholds (one-sample two-sided sign test and FDR-adjusted $*p < 0.000001$) (Figure 4C, 75%, top; 87.5%, bottom). As we adjusted the OCD-detection threshold from 75% to 87.5%, rDBS detection count per day significantly decreased ($*p < 0.00001$, two-sample one-sided Wilcoxon rank sum test; Figure S4). Assuming a minimum 1 s stimulation duration for each stimulation, rDBS at 75% detection threshold delivers a minimum of 814 s (median daily detection count = 814/day \times

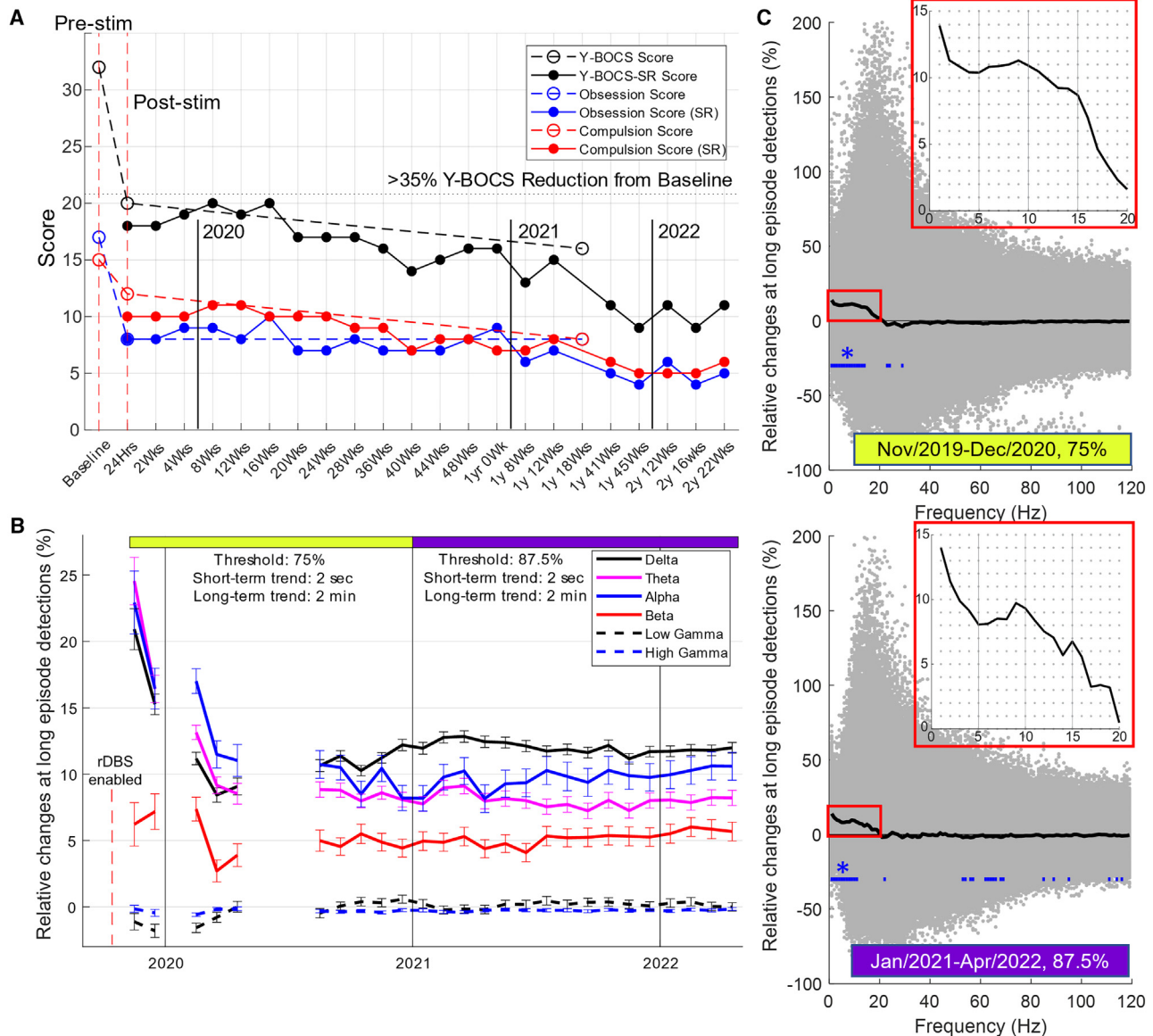


Figure 4. rDBS therapeutic outcomes

(A) Y-BOCS, obsessive, and compulsive scores over time. Y-BOCS scores of the baseline, and 24 h and 1 year 18 weeks post-NAc-VeP-rDBS activation were assessed by the clinician. Y-BOCS-SR was reported over the 2 years 22 weeks after surgery (biweekly, first month, intermittently afterward). Y-BOCS decreased rapidly and durably after rDBS was enabled.

(B) Relative changes of the absolute power at long-episode detections (AUC peaks) from the average across the month (mean \pm SEM). The relative change is calculated for each detection as short-term trend/long-term trend of absolute power. Two different detection settings are depicted by yellow and purple; blanks are no data with those detection settings. The frequency band with the most increased power was delta in 2021–2022 (purple).

(C) Relative changes at long-episode detections in (B) across the frequency. All the relative power as gray dots across the frequency when rDBS detection was activated. The median of the relative power within the same frequency is depicted with a black solid line. The median of the low-frequency (<11 Hz) power is significantly greater than zero in both detection settings depicted with a blue solid line (one-sample two-sided sign test, and FDR-adjusted $*p < 0.000001$). When rDBS detection is enabled by AUC detector, the median of delta-frequency power was the highest compared with its average.

1 s stimulation) of stimulation daily. Assuming 24-h bursting for conventional continuous DBS, rDBS delivers 99.06% less stimulation than conventional continuous DBS. Calculated at 87.5% threshold, rDBS delivers a minimum of 530 s of stimulation (median daily detection count = 530/day \times 1 s stimulation), which is 99.39% less than the continuous DBS. Each OCD detection

could result in up to 4 subsequent detections at both sides, resulting in a maximum of 5 OCD stimulations (stimulation from the initial detection + 4 subsequent detections) and 4 epilepsy stimulations. As such, a maximum duration of stimulation could be calculated. Epilepsy stimulation was delivered for a median of 251 s/day (75% threshold) and 394 s/day (87.5% threshold). At

75% detection threshold, a maximum of 5,074 s of Nac-VeP stimulation (814 s/day from OCD detection*5 + 251 s/day from epilepsy detection*4) is delivered per day—still 94.13% less than the continuous DBS. For 87.5% threshold, a maximum of 4,226 s of stimulation (530 s/day from OCD detection*5 + 394 s/day from epilepsy detection*4) is delivered per day—95.11% less than the continuous DBS (Figure S4). To examine the degree of temporal co-occurrence between OCD and seizure-triggered stimulation, we quantified how often detection-triggered OCD stimulation and epilepsy stimulation occurred within 20 s of each other. Our analyses suggested the total percent of co-occurrence between OCD and seizure-triggered stimulation is 1.66%. For the threshold of 75%, it is 0.32%. For 87.5%, it is 2.49%. These findings suggest minimal co-occurrence in the delivery of the two stimulations for this patient.

DISCUSSION

Our study identified an association between Nac-VeP low-frequency oscillatory power and obsessions characteristic of OCD. We used the detection of above-threshold AUC in the iEEG found to be driven by low-frequency power to trigger stimulation of these specific ventral striatal regions in a single subject with trOCD. Clinically, the patient's symptom severity reported both subjectively and objectively (Y-BOCS) was substantially improved (37.5% acute decrease post-stimulation) with rDBS. This highlights that disrupting the Nac-VeP, specifically during the presence of a signal found to be related to obsessions, blunted the urge to compulsive. Symptom-locked ambulatory electrophysiologic data, as well as in-lab provocation tasks, all found AUC for low-frequency oscillations to be elevated during obsessive states. To validate the ambulatory and lab-based findings, signals locked to the detections themselves were analyzed, and low-frequency power was again found to be the most prominent frequency contributing to above-threshold AUC elevations triggering a detection. It is important to note that the peaks above a 65% threshold in the VR provocation task analyses were only found in the high distress trials, further evidencing the relevance of this metric to OCD-related distress. The patient only reported the distress level with a few sample sizes of -3 ($n = 3$) and -2 ($n = 8$); hence, the comparison of high vs. low distress should be interpreted with caution. A powerful analysis would have been to correlate obsessive symptom severity with spectral power during ambulatory obsessive snapshots. Student's *t* test for each frequency revealed a non-significant difference between high or low SUDS vs. control and high vs. low SUDS. However, due to the limited sample size of patient-reported symptom ratings ($n = 7$), inferences from this statistical result should be made with caution.

There were some analytic and experimental challenges encountered in this study. First, as it relates to our findings, there were inconsistencies between ambulatory and in-lab provocation task-related findings. Specifically, the ambulatory findings suggested <15 Hz power to associate with obsessions, whereas in-lab provocation task-related data evidenced relevance for only <4 Hz power. Although there is an overlap in the delta range between the ambulatory and in-lab provocation tasks, there were some key discrepancies between them that could

contribute to a broader low-frequency range in ambulatory data. Most critically, the ambulatory recordings were: (1) capturing iEEG during spontaneous, naturalistic obsessions (although provocation tasks were provoking obsessions using distressing items); (2) capturing data over a greater duration of time; and (3) specifically time-locked to moments of obsessions, whereas the provocation task data was confounded by simultaneous interaction with those items. There were also discrepancies in the thresholds maximizing specificity between the real world ($P_{>35}$) and VR ($P_{>50}$) that could be explained by the higher amplitude peaks in the VR neutral trials. The naturalistic provocation task did acquire more time after interaction (>5 min) with obsessive trials. As the VR provocation task provided less time between trials for patients to return to baseline, it is possible that neutral trials were confounded by the heightened obsessive state induced by prior trials. It is worth noting that almost every obsessive episode in ambulatory task was followed by a compulsion, making it difficult to disentangle the relevance of our results to obsessive- vs. compulsive-related behaviors. However, as the ambulatory signal was captured during obsessive thoughts, preceding the onset of compulsive behavior, we hypothesize that this signal found in our results is likely indexing obsessive thought or the urge to compulsive. This generalizes to the provocation task signals as well, as it specifically reflects signal during active obsessive thought, in the absence of subsequent compulsion. Importantly, both task and ambulatory data demonstrate the relevance of low-frequency power, suggesting an overlap in the underlying symptoms driving these signals in both settings. It is an important observation that in an exploratory analysis, Y-BOCS scores (symptom severity in the last 7 days) positively correlated with low-frequency power (averaged across 7 days preceding Y-BOCS completion) (Figure S3C). This low-frequency power was specific and limited to long-episode detections. The findings of this analysis are further limited as the saved iEEG data from which we generated the dataset accounts for a very small percentage of daily detections (~ 3 /day vs. >500 /day), necessitating caution in its interpretation.

There were also some analytic inconsistencies between provocation tasks and AUC detection algorithm in the rDBS system. The first relates to how short- and long-term trends were calculated between provocation tasks. In calculating the spectral contributions to AUC detections, we used a 90-s average instead of the 120-s (rDBS) detection long-term trend. For the ambulatory iEEG data, we calculated the long-term trend using the 60 s prior to swipe, as we did not have the full 120-s long-term data used in the AUC detection algorithm. Importantly, at a detection threshold of 75%, although specificity was maximal, sensitivity was not. In our analytic investigation, we can retrospectively identify that a detection threshold of 30% would have maximized the sum of sensitivity and specificity for this patient. Future work should run similar analytic interrogations of an optimized detection threshold to inform individualized stimulation settings. The responsive DBS strategy is delivered based on the time-domain feature (AUC) that is intrinsic to the device. Finally, it is important to note that the detection threshold for this patient was changed from 75% in 2019 to 87.5% in 2021. The clinicians made this adjustment as an attempt to balance the number of seizure

snapshots from the temporal lobe and obsessive detection snapshots from the NAc-VeP being recorded due to storage limitations of the NeuroPace device. This was driven by an initial imbalance favoring large numbers of obsessive detections, resulting in seizure iEEG events being overwritten. Detection algorithms for the rDBS device could be better optimized for OCD, for example, through the implementation of online machine learning algorithms. However, the current device is limited in computing capacity, which prohibits the incorporation of more advanced online analytics.

Regarding the DBS target, the electrode contacts are 10-mm spaced from center to center, which makes definitively attributing results to either the VeP or NAc difficult. This limitation is inherent to most human DBS studies of this region, which do not attempt to delineate subregions within the ventral striatum. The most ventral contact is in the ventral border of the NAc, which is proximal (about 3 mm) to the ventral prefrontal regions broadly implicated in psychiatric disorders, such as OCD and depression.²⁵ As it is difficult to know the boundary of our bipolar stimulation field, this ventral frontal region may indeed have received charge density from nearby stimulation bouts, which may in part have been therapeutic as this NAc-mPFC circuit relates to impulse control as found in our prior work.²⁶ This limitation, however, may be common to all ventral striatal DBS outcomes given the proximity of the NAc to this cortical node. Furthermore, we recorded from and stimulated only the right NAc-VeP. Unilateral NAc region DBS has been found to be efficacious in tOCD, and although it is likely that bilateral implants are more efficacious, the surgeon appropriately decided to prioritize safety, confirm feasibility, and assess initial efficacy of this off-label case. Finally, treatment was delivered open-label and without control conditions, although the durable, long-term therapeutic effect reported here in a severe OCD patient is notable, particularly given the smaller placebo effects observed in this population.^{27–29} Finally, after 5 months, detection power stabilized, but symptoms continued to improve. Therefore, it is worth noting that there are contributions to longer-term clinical improvement outside of detections that were not captured or controlled for this patient. Another important observation is that the frequency of detections (detection count) and, therefore, the frequency of stimulation were relatively stable over time and did not correlate with the Y-BOCS clinical outcome. This is despite a decrease in power of low-frequency rhythms. We hypothesize that signal triggering a detection is the neurophysiological signal of interest capturing a neural state related to OCD symptoms. However, immediate intervention in response to detections (i.e., responsive stimulation or rDBS) is intended to reduce symptoms associated with that neurophysiological signal of interest—not to prevent the occurrence of that signal per se. It is thus not surprising that in the setting of active rDBS, the frequency of this neurophysiological signal of interest (detection count) does not correlate with symptom severity over time, as measured by the Y-BOCS. Importantly, the decrease in the low-frequency power associated with long-episode detections indicates that although AUC increases were still robust enough to exceed the detection threshold, the lower-frequency contributions to these detections did decrease over time and are perhaps a more sensitive metric for symptom severity than AUC increases alone.

It is important to mention that although this work may pave the way to a new line of research into OCD and closed-loop neurostimulation techniques, the generalizability is limited by a number of factors, including that this is a single patient, this patient had comorbid epilepsy, and the DBS trajectory was novel with additional active electrodes outside the NAc-VeP zone. Additionally, the novel parietal DBS trajectory traversed the external segment of the globus pallidus, which theoretically could have affected OCD symptoms, particularly if GPi was inadvertently modulated.³⁰ However, the patient's implant surgery was 7 months prior to initiating stimulation to her OCD electrode, and the OCD Y-BOCS was stable during her epilepsy treatment (which included external globus pallidus stimulation due to peri-insular lead location). Her OCD only began to decrease after responsive NAc-VeP stimulation was enabled following the epilepsy treatment (at no time was NAc-VeP stimulated prior to the patient's OCD treatment initiation). Therefore, it is unlikely that seizure-targeted neurostimulation, nor the impact of this trajectory, accounts for the DBS-related improvement reported in this manuscript. However, it is impossible to rule out the chance that the OCD therapy contributed to the patient's epilepsy improvement or the chance that the epilepsy therapy contributed to the patient's OCD improvement. Although the trajectory conveys a potential limitation in generalizability, we do want to note that this novel trajectory allows for the NAc and VeP to be modulated, as it still remains unclear which part of the ventral striatum is mediated in therapeutic DBS cases. It is important to re-emphasize that only the electrodes detecting the biomarker activation (above-threshold AUC peaks) delivered stimulation. Furthermore, there was no therapeutic comparison of our responsive DBS against conventional or adaptive DBS, as this would not be possible with the implanted device. Finally, as the patient was being treated simultaneously for comorbid OCD and epilepsy, detection settings had to be adjusted to balance the number of seizure and obsession-related detection snapshots being recorded due to storage limitations of the device. Specifically, the threshold for detections was determined with consideration of both epilepsy and OCD-related physiology. The detection threshold was changed from 75% OCD threshold to 87.5% OCD threshold to account for the shared storage space between epilepsy and OCD long-episode detection iEEG data and better equilibrate OCD vs. epilepsy iEEG data storage. At 75% detection threshold (7/30/2020–1/14/2021), 960 long-episode detection iEEG OCD snapshots were stored compared with 64 long-episode detection iEEG epilepsy snapshots (0.067 epilepsy/OCD ratio). At 87.5% detection threshold (1/15/2021–7/03/2022), 790 long-episode detection iEEG OCD snapshots were stored compared with 920 long-episode detection iEEG epilepsy snapshots (1.168 epilepsy/OCD ratio). Psychiatric comorbidities are very common in epilepsy (up to 22%³¹), and therefore, it is important to evaluate efficacy in patient populations with comorbidities while also being a critical step forward to the translation of this potential treatment to primary psychiatric conditions.^{32,33} All these points are important considerations affecting the generalizability of the current manuscript's findings. This case presents evidence that these issues can be treated in parallel and relevant physiology can be dissociated. Whether the findings of this case can generalize to OCD in the absence of epilepsy remains unknown but subject to future testing.

In conclusion, we present the first-in-human trial of a closed-loop DBS approach to treat obsessive symptoms in OCD. Furthermore, we validate the relevance of AUC measurements on a low-frequency spectral basis to OCD symptoms via signals recorded during ambulatory symptom presentation, in-lab provocation tasks, and rDBS detections. This study suggests ventral striatal rDBS may be a promising and novel intervention for OCD.

STAR★METHODS

Detailed methods are provided in the online version of this paper and include the following:

- **KEY RESOURCES TABLE**
- **RESOURCE AVAILABILITY**
 - Lead contact
 - Materials availability
 - Data and code availability
- **METHOD DETAILS**
 - Pre-study procedures
 - rDBS signal identification
 - Analyses
 - rDBS programming
 - rDBS therapeutic outcomes

SUPPLEMENTAL INFORMATION

Supplemental information can be found online at <https://doi.org/10.1016/j.neuron.2023.09.034>.

ACKNOWLEDGMENTS

This work was supported by the National Institute of Health (5UH3NS103446-02 and U01NS117838 to C.H.H.) and the Foundation for OCD Research to C.H.H., and N.R.W. C.E.R. was supported by 5F32MH127859-03. The authors thank the study subject for their dedication and commitment to this novel, first-in-human exploratory case; the members of the Stanford Clinical and Translational Research Unit and the Departments of Neurosurgery and Psychiatry at Stanford Medicine for space to conduct in-clinic assessments; the Suthana laboratory for in-clinic tool support; Vyvian Ngo and Bharati Sanjanwala for support during follow-up periods; and Emily Mirro, Tara L. Skarpaas, Nick Hasulak, and Tom Tchong for providing technical support for the NeuroPace RNS System. Thank you to Dr. Edna Foa and Dr. Lily Brown for their intellectual contributions to our understanding of obsessive-compulsive disorder and the clinical framework to interpret our results within.

AUTHOR CONTRIBUTIONS

Y.-H.N., C.E.R., R.S.S., D.A.N.B., and C.H.H. wrote the manuscript with invaluable input from all authors. R.S.S., U.T., T.N.C., S.H., A.F., and D.A.N.B. conducted clinical and electrophysiological data collection. D.B. designed and executed the VR provocation task. F.M.E., I.H.K., N.R.W., R.S.S., and D.A.N.B. designed the real-world provocation task. Y.-H.N., C.E.R., D.B., J.G., R.S.S., B.P., and D.J.O. conducted data analyses. A.M.R. performed the surgical procedure, and M.K. managed the subject's epilepsy treatment. C.H.H. and M.T.B. managed the subject's OCD treatment. C.H.H. provided supervision and guidance throughout the study. N.S. and C.H.H. provided financial support to conduct this case report.

DECLARATION OF INTERESTS

No funding from NeuroPace was received for this study nor were data analyses reported here conducted by NeuroPace employees. C.H.H., R.S.S., and C.E.R. have patents related to sensing and brain stimulation for the treatment

of neuropsychiatric disorders. C.H.H. is a consultant for Boston Scientific and Insightec and receives honoraria for educational lectures.

Received: February 13, 2023

Revised: August 12, 2023

Accepted: September 26, 2023

Published: October 20, 2023

REFERENCES

1. Mancebo, M.C., Eisen, J.L., Grant, J.E., and Rasmussen, S.A. (2005). Obsessive compulsive personality disorder and obsessive compulsive disorder: clinical characteristics, diagnostic difficulties, and treatment. *Ann. Clin. Psychiatry* *17*, 197–204. <https://doi.org/10.1080/10401230500295305>.
2. Stein, D.J., Costa, D.L.C., Lochner, C., Miguel, E.C., Reddy, Y.C.J., Shavitt, R.G., van den Heuvel, O.A., and Simpson, H.B. (2019). Obsessive-compulsive disorder. *Nat. Rev. Dis. Primers* *5*, 52. <https://doi.org/10.1038/s41572-019-0102-3>.
3. Ruscio, A.M., Stein, D.J., Chiu, W.T., and Kessler, R.C. (2010). The epidemiology of obsessive-compulsive disorder in the National Comorbidity Survey Replication. *Mol. Psychiatry* *15*, 53–63. <https://doi.org/10.1038/mp.2008.94>.
4. Foa, E.B. (2010). Cognitive behavioral therapy of obsessive-compulsive disorder. *Dial. Clin. Neurosci.* *12*, 199–207. <https://doi.org/10.31887/DCNS.2010.12.2/efoa>.
5. Carmi, L., Tendler, A., Bystritsky, A., Hollander, E., Blumberger, D.M., Daskalakis, J., Ward, H., Lapidus, K., Goodman, W., Casuto, L., et al. (2019). Efficacy and safety of deep transcranial magnetic stimulation for obsessive-compulsive disorder: A prospective multicenter randomized double-blind placebo-controlled trial. *Am. J. Psychiatry* *176*, 931–938. <https://doi.org/10.1176/appi.ajp.2019.18101180>.
6. Liang, K., Li, H., Bu, X., Li, X., Cao, L., Liu, J., Gao, Y., Li, B., Qiu, C., Bao, W., et al. (2021). Efficacy and tolerability of repetitive transcranial magnetic stimulation for the treatment of obsessive-compulsive disorder in adults: a systematic review and network meta-analysis. *Transl. Psychiatry* *11*, 332. <https://doi.org/10.1038/s41398-021-01453-0>.
7. Nakao, T. (2013). Treatment-refractory OCD and its biological pathophysiology. *Seishin Shinkeigaku Zasshi* *115*, 981–989.
8. Del Casale, A., Sorice, S., Padovano, A., Simmaco, M., Ferracuti, S., Lamis, D.A., Rapinesi, C., Sani, G., Girardi, P., Kotzalidis, G.D., and Pompili, M. (2019). Psychopharmacological treatment of obsessive-compulsive disorder (OCD). *Curr. Neuropharmacol.* *17*, 710–736. <https://doi.org/10.2174/1570159X16666180813155017>.
9. Kumar, K.K., Appelboom, G., Lamsam, L., Caplan, A.L., Williams, N.R., Bhati, M.T., Stein, S.C., and Halpern, C.H. (2019). Comparative effectiveness of neuroablation and deep brain stimulation for treatment-resistant obsessive-compulsive disorder: a meta-analytic study. *J. Neurol. Neurosurg. Psychiatry* *90*, 469–473. <https://doi.org/10.1136/jnnp-2018-319318>.
10. Wu, H., Kakusa, B., Neuner, S., Christoffel, D.J., Heifets, B.D., Malenka, R.C., and Halpern, C.H. (2022). Local accumbens in vivo imaging during deep brain stimulation reveals a strategy-dependent amelioration of hedonic feeding. *Proc. Natl. Acad. Sci. USA* *119*, e2109269118. <https://doi.org/10.1073/pnas.2109269118>.
11. Hartshorn, A., and Jobst, B. (2018). Responsive brain stimulation in epilepsy. *Ther. Adv. Chronic Dis.* *9*, 135–142. <https://doi.org/10.1177/2040622318774173>.
12. Scangos, K.W., Khambhati, A.N., Daly, P.M., Makhoul, G.S., Sugrue, L.P., Zamanian, H., Liu, T.X., Rao, V.R., Sellers, K.K., Dawes, H.E., et al. (2021). Closed-loop neuromodulation in an individual with treatment-resistant depression. *Nat. Med.* *27*, 1696–1700. <https://doi.org/10.1038/s41591-021-01480-w>.
13. Heck, C.N., King-Stephens, D., Massey, A.D., Nair, D.R., Jobst, B.C., Barkley, G.L., Salanova, V., Cole, A.J., Smith, M.C., Gwinn, R.P., et al.

- (2014). Two-year seizure reduction in adults with medically intractable partial onset epilepsy treated with responsive neurostimulation: final results of the RNS System Pivotal trial. *Epilepsia* 55, 432–441. <https://doi.org/10.1111/epi.12534>.
14. Razavi, B., Rao, V.R., Lin, C., Bujarski, K.A., Patra, S.E., Burdette, D.E., Geller, E.B., Brown, M.M., Johnson, E.A., Drees, C., et al. (2020). Real-world experience with direct brain-responsive neurostimulation for focal onset seizures. *Epilepsia* 61, 1749–1757. <https://doi.org/10.1111/epi.16593>.
 15. Miller, K.J., Burns, T.C., Grant, G.A., and Halpern, C.H. (2015). Responsive stimulation of motor cortex for medically and surgically refractive epilepsy. *Seizure* 33, 38–40. <https://doi.org/10.1016/j.seizure.2015.10.011>.
 16. Shivacharan, R.S., Rolle, C.E., Barbosa, D.A.N., Cunningham, T.N., Feng, A., Johnson, N.D., Safer, D.L., Bohon, C., Keller, C., Buch, V.P., et al. (2022). Pilot study of responsive nucleus accumbens deep brain stimulation for loss-of-control eating. *Nat. Med.* 28, 1791–1796. <https://doi.org/10.1038/s41591-022-01941-w>.
 17. Rappel, P., Marmor, O., Bick, A.S., Arkadir, D., Linetsky, E., Castrioto, A., Tamir, I., Freedman, S.A., Mevorach, T., Gilad, M., et al. (2018). Subthalamic theta activity: a novel human subcortical biomarker for obsessive compulsive disorder. *Transl. Psychiatry* 8, 118. <https://doi.org/10.1038/s41398-018-0165-z>.
 18. Alhourani, A., McDowell, M.M., Randazzo, M.J., Wozny, T.A., Kondylis, E.D., Lipski, W.J., Beck, S., Karp, J.F., Ghuman, A.S., and Richardson, R.M. (2015). Network effects of deep brain stimulation. *J. Neurophysiol.* 114, 2105–2117. <https://doi.org/10.1152/jn.00275.2015>.
 19. Miller, K.J., Prieto, T., Williams, N.R., and Halpern, C.H. (2019). Case Studies in Neuroscience: The electrophysiology of a human obsession in nucleus accumbens. *J. Neurophysiol.* 121, 2336–2340. <https://doi.org/10.1152/jn.00096.2019>.
 20. Goodman, W.K., Price, L.H., Rasmussen, S.A., Mazure, C., Fleischmann, R.L., Hill, C.L., Heninger, G.R., and Charney, D.S. (1989). The Yale-Brown Obsessive Compulsive Scale. I. Development, use, and reliability. *Arch. Gen. Psychiatry* 46, 1006–1011. <https://doi.org/10.1001/archpsyc.1989.01810110048007>.
 21. Goodman, W.K., Price, L.H., Rasmussen, S.A., Mazure, C., Delgado, P., Heninger, G.R., and Charney, D.S. (1989). The Yale-Brown Obsessive Compulsive Scale. II. Validity. *Arch. Gen. Psychiatry* 46, 1012–1016. <https://doi.org/10.1001/archpsyc.1989.01810110054008>.
 22. Federici, A., Summerfeldt, L.J., Harrington, J.L., McCabe, R.E., Purdon, C.L., Rowa, K., and Antony, M.M. (2010). Consistency between self-report and clinician-administered versions of the Yale-Brown Obsessive-Compulsive Scale. *J. Anxiety Disord.* 24, 729–733. <https://doi.org/10.1016/j.janxdis.2010.05.005>.
 23. Rapp, A.M., Bergman, R.L., Piacentini, J., and McGuire, J.F. (2016). Evidence-based assessment of obsessive-compulsive disorder. *J. Cent. Nerv. Syst. Dis.* 8, 13–29. <https://doi.org/10.4137/JCNSD.S38359>.
 24. Huff, W., Lenartz, D., Schormann, M., Lee, S.H., Kuhn, J., Koulousakis, A., Mai, J., Daumann, J., Maarouf, M., Klosterkötter, J., and Sturm, V. (2010). Unilateral deep brain stimulation of the nucleus accumbens in patients with treatment-resistant obsessive-compulsive disorder: Outcomes after one year. *Clin. Neurol. Neurosurg.* 112, 137–143. <https://doi.org/10.1016/j.clineuro.2009.11.006>.
 25. Huey, E.D., Zahn, R., Krueger, F., Moll, J., Kapogiannis, D., Wassermann, E.M., and Grafman, J. (2008). A psychological and neuroanatomical model of obsessive-compulsive disorder. *J. Neuropsychiatry Clin. Neurosci.* 20, 390–408. <https://doi.org/10.1176/jnp.2008.20.4.390>.
 26. Barbosa, D.A.N., Kuijper, F.M., Duda, J., Wang, A.R., Cartmell, S.C.D., Saluja, S., Cunningham, T., Shivacharan, R.S., Bhati, M.T., Safer, D.L., et al. (2022). Aberrant impulse control circuitry in obesity. *Mol. Psychiatry* 27, 3374–3384. <https://doi.org/10.1038/s41380-022-01640-5>.
 27. Sugarman, M.A., Kirsch, I., and Huppert, J.D. (2017). Obsessive-compulsive disorder has a reduced placebo (and antidepressant) response compared to other anxiety disorders: A meta-analysis. *J. Affect. Disord.* 218, 217–226. <https://doi.org/10.1016/j.jad.2017.04.068>.
 28. Mohamadi, S., Ahmadzad-Asl, M., Nejadghaderi, S.A., Jabbarinejad, R., Mirbehbahani, S.H., Sinyor, M., Richter, M.A., and Davoudi, F. (2023). Systematic review and meta-analysis of the placebo effect and its correlates in obsessive compulsive disorder. *Can. J. Psychiatry* 68, 479–494. <https://doi.org/10.1177/07067437221115029>.
 29. Kotzalidis, G.D., Del Casale, A., Simmaco, M., Pancheri, L., Brugnoli, R., Paolini, M., Gualtieri, I., Ferracuti, S., Savoia, V., Cuomo, I., et al. (2019). Placebo effect in obsessive-compulsive disorder (OCD). Placebo response and placebo responders in OCD: The trend over time. *Curr. Neuropharmacol.* 17, 741–774. <https://doi.org/10.2174/1570159X16666181026163922>.
 30. Johnson, K.A., Duffley, G., Foltynie, T., Hariz, M., Zrinzo, L., Joyce, E.M., Akram, H., Servello, D., Galbiati, T.F., Bona, A., et al. (2021). Basal ganglia pathways associated with therapeutic pallidal deep brain stimulation for Tourette syndrome. *Biol. Psychiatry Cogn. Neurosci. Neuroimaging* 6, 961–972. <https://doi.org/10.1016/j.bpsc.2020.11.005>.
 31. Mula, M., Pini, S., Monteleone, P., Iazzetta, P., Preve, M., Tortorella, A., Amato, E., Di Paolo, L., Conversano, C., Rucci, P., et al. (2008). Different temperament and character dimensions correlate with panic disorder comorbidity in bipolar disorder and unipolar depression. *J. Anxiety Disord.* 22, 1421–1426. <https://doi.org/10.1016/j.janxdis.2008.02.004>.
 32. Davis, R.A., Winston, H., Gault, J.M., Kern, D.S., Mikulich-Gilbertson, S.K., and Abosch, A. (2021). Deep brain stimulation for OCD in a patient with comorbidities: Epilepsy, tics, autism, and major depressive disorder. *J. Neuropsychiatry Clin. Neurosci.* 33, 167–171. <https://doi.org/10.1176/appi.neuropsych.20060153>.
 33. Kahn, L., Sutton, B., Winston, H.R., Abosch, A., Thompson, J.A., and Davis, R.A. (2021). Deep brain stimulation for obsessive-compulsive disorder: Real world experience post-FDA-humanitarian use device approval. *Front. Psychiatry* 12, 568932. <https://doi.org/10.3389/fpsy.2021.568932>.
 34. Cartmell, S.C.D., Miller, K.J., Ho, A.L., and Halpern, C.H. (2018). Frameless stereotactic dual lead placement through single burr hole: a technical report. *J. Clin. Neurosci.* 55, 100–102. <https://doi.org/10.1016/j.jocn.2018.06.053>.
 35. Blumer, D., Wakhlu, S., Davies, K., and Hermann, B. (1998). Psychiatric outcome of temporal lobectomy for epilepsy: incidence and treatment of psychiatric complications. *Epilepsia* 39, 478–486. <https://doi.org/10.1111/j.1528-1157.1998.tb01409.x>.
 36. Koch-Weser, M., Garron, D.C., Gilley, D.W., Bergen, D., Bleck, T.P., Morrell, F., Ristanovic, R., and Whisler, W.W., Jr. (1988). Prevalence of psychologic disorders after surgical treatment of seizures. *Arch. Neurol.* 45, 1308–1311. <https://doi.org/10.1001/archneur.1988.00520360026006>.
 37. Halpern, C.H., Santini, V., Lipsman, N., Lozano, A.M., Schwartz, M.L., Shah, B.B., Elias, W.J., Cosgrove, G.R., Hayes, M.T., McDannold, N., et al. (2019). Three-year follow-up of prospective trial of focused ultrasound thalamotomy for essential tremor. *Neurology* 93, e2284–e2293. <https://doi.org/10.1212/WNL.00000000000008561>.
 38. Morrell, M.J.; RNS System in Epilepsy Study Group (2011). Responsive cortical stimulation for the treatment of medically intractable partial epilepsy. *Neurology* 77, 1295–1304. <https://doi.org/10.1212/WNL.0b013e3182302056>.
 39. Topalovic, U., Aghajan, Z.M., Villaroman, D., Hiller, S., Christov-Moore, L., Wishard, T.J., Stangl, M., Hasulak, N.R., Inman, C.S., Fields, T.A., et al. (2020). Wireless programmable recording and stimulation of deep brain activity in freely moving humans. *Neuron* 108, 322–334.e9. <https://doi.org/10.1016/j.neuron.2020.08.021>.

STAR★METHODS

KEY RESOURCES TABLE

REAGENT or RESOURCE	SOURCE	IDENTIFIER
Software and algorithms		
MATLAB R2021b	The MathWorks	https://www.mathworks.com/products/matlab.html
Unity 2018.4.14f1	Unity Technologies	https://unity.com/releases/editor/archive
FieldTrip 2021.10.20	FieldTrip toolbox	https://www.fieldtriptoolbox.org/
Other		
RNS-320	NeuroPace	https://www.neuropace.com/providers/rns-system-neuromodulation/

RESOURCE AVAILABILITY

Lead contact

Further information and requests for resources and results should be directed to the lead contact Casey H. Halpern (casey.halpern@penmedicine.upenn.edu).

Materials availability

Raw data, including electrophysiology and CT/MRI images, that are newly collected in this study are not publicly available due to them containing information that could compromise research participant privacy/consent, but they can be shared privately upon request.

Data and code availability

Any additional information and codes required to reanalyze the data reported in this paper are available from the [lead contact](#) upon request.

METHOD DETAILS

Pre-study procedures

At the time of this task, the patient was a 31-year-old female with a history of OCD and comorbid temporal lobe epilepsy. The patient described significant impairment of her daily functioning due to her OCD symptoms, especially those concerned with safety (both for herself and those close to her) and food contamination. She underwent a number of psychological and pharmacological treatments for OCD with limited to no benefit, including six months of cognitive behavioral therapy, exposure response prevention, and multiple antidepressants. The patient had had a prior anterior temporal lobectomy. At the time of this study, she was taking stable doses of sertraline and several anticonvulsant medications with limited benefit. The patient underwent placement of the two leads of rDBS System targeting the right NAc-VeP region and right temporal lobe, the latter was based on her invasive seizure monitoring data (Figures 1A and S1). The patient's implant surgery to treat a seizure was 7 months prior to initiating stimulation for OCD, and rDBS for a seizure was enabled after the surgery. Using standard stereotactic surgery procedures, and co-registration of MRI and CT images, the right NAc-VeP ventral striatal lead's most distal contact was placed targeting contact 1 to the NAc at its depth (most anteriorly) and contact 2 up to the posterior border of the VeP (border of the Anterior Commissure) (Figure 1A). Since a burr hole was already created to target the temporal lobe to treat epilepsy, a novel surgical trajectory traversing the ventral striatal territories implicated in OCD was chosen to minimize invasiveness of the procedure as previously reported using the existing burr hole.³⁴ This right NAc-VeP lead was placed off-label in an attempt to treat OCD (comorbid to her epilepsy), given how refractory both her epilepsy and OCD were, and the severe disability caused by both conditions. Moreover, psychopathology involving OCD has been reported to worsen following epilepsy surgery, thus advancing this depth electrode to the NAc-VeP was intended to better prepare this patient's treatment team and spare her another intracranial procedure (i.e., conventional DBS).^{35,36} Electrode location was confirmed after lead reconstruction using the postoperative CT scan co-registered to preoperative MRI. NAc-VeP masks are included for illustrative purposes only using previously described methods.²⁶

At the time of initiating physiologic biomarker discovery for personalized obsessions, the patient was taking stable doses of sertraline and was 6-months status post implantation when stimulation was activated on the temporal lead alone. This patient's comorbid epilepsy was thus treated (for 7 months following implant surgery) and stabilized prior to initiating the OCD-specific intervention

here, and this effect was sustained and managed as standard of care in parallel to the effort reported in more detail here. Briefly, she exhibited ~60% improvement in seizure frequency (data is not shown but is customary for this standard treatment) aligned to prior publications of responsive neurostimulation outcomes for epilepsy,^{37,38} and her trOCD was reported to have been unchanged up until the time of initiating rDBS targeted to her obsessions. All study procedures described below were reviewed and approved by the Institutional Review Board at Stanford University (IRB #33146). This study was conducted prospectively during the implementation of this off-label, first-in-human treatment for trOCD.

rDBS signal identification

Ambulatory task

The patient was given a home data-collection triggering magnet (NeuroPace Magnet, Model M-02), allowing the patient to initiate iEEG snapshot recordings in the ambulatory setting for a pre-specified duration (3 min) by swiping the magnet over her neurostimulator. She was instructed to initiate such recordings when she experienced obsessive thoughts around her safety, prior to beginning her compulsion (e.g., checking doors, windows, and appliances), or if she was feeling especially asymptomatic (control). She was also instructed to maintain a log on how she felt during each recording, detailing any symptoms, noting the time, level of distress, and what she was doing. There were 35 obsessions and 10 control snapshots.

In-lab naturalistic provocation task

Using novel tools to synchronize and to allow patients to freely move with the implanted system,³⁹ we provoked contamination obsessions via exposure to personalized distressing foods and measured the associated levels of distress. There were four distinct phases of this provocation task: Anticipation, Viewing, Interaction, and Rating. The subject awaited a door knock to signal the delivery of the next item (Anticipation). A researcher then delivered the item to the tray directly in front of the subject (Viewing). The subject then has the option of interacting with that item (Interaction), the duration of which was 16-78 s (Figure 2A, top). Finally, the subject rated the current SUDS, from 0 to 100 (Rating). Two categories of trials were administered - 1) “neutral” trials: delivery of neutral items (e.g., newspaper), and 2) “obsessive trials”: delivery of provocative items (e.g., shrimp). There was a total of 18 trials, 7 of which were provocative; 11 of which were neutral. The experiment was performed for 3 days, and the order of each item was randomly shuffled. Neutral items (items that did not provoke OCD-related distress) were contrasted against obsessive items (items that did provoke OCD-related distress). SUDS during this task were rated on a distress level of 0-100, in real-time, during item presentation. Neutral trials had SUDS ratings of 10.18 ± 0.18 , and obsessive trials had SUDS ratings of 32.86 ± 2.86 (mean \pm SEM) which is a significant elevation from neutral trials (* $p < 0.0000001$, two-sample two-sided Student’s t test). For obsessive trials, items used were previously mentioned by the patient that provoke obsessive thoughts and/or an urge to compulsive. SUDS ratings were recorded, and, not surprisingly, were associated with the highest experience of distress specific to interaction with the obsessive items compared to neutral items (SUDS: 57.86 ± 4.06 , mean \pm SEM). The interaction resulted in a significant increase in SUDS in interaction compared to the presentation (* $p = 0.00029$, two-sample two-sided Student’s t test).

In-lab VR provocation task

Using novel tools to synchronize and to allow the participant to freely move with the implanted system,³⁹ the patient completed laboratory tasks to identify changes in electrophysiology associated with her contamination obsessions surrounding seafood (Figure 2A, bottom). There were four distinct phases of this provocation task: Anticipation, Viewing, Interaction, and Rating. During anticipation a green light signaled the category of item that was to be presented. The item then proceeded towards the center of the screen over the course of 8-14 s. The subject then has the option of interacting with that item, the duration of which was 2-3 s. Finally, the subject rated her discomfort level, from -3 (very distressful) to 3 (very comfortable). Two categories of trials were compared - 1) “neutral” trials: delivery of neutral items, and 2) “obsessive trials”: delivery of provocative items (e.g., seafood). There was a total of 22 trials, 11 of which were provocative, and 11 of which were neutral. Neutral items (items that did not provoke OCD-related distress, and were recorded 0 ± 0) were contrasted against obsessive items (items that were associated with OCD-related distress). For obsessive items, these are items that, when encountered by the patient, provoke obsessive thoughts and/or an urge to compulsive. Distress level ratings were recorded, and corroborated highest experiences of distress specific to interaction with the obsessive items (Distress: -2.27 ± 0.14 , mean \pm SEM) which was significantly different from the neutral item (* $p < 0.0000001$, two-sample two-sided Student’s t test).

Analyses

The below analyses were conducted on iEEG data from 3 data streams: 1) Ambulatory data snapshots (obsessions, control snapshots) 2) Provocation tasks: naturalistic provocation task, VR provocation task (Obsessive, neutral trials), and 3) Detection data snapshots.

AUC

The rDBS system triggers stimulation based on elevations in AUC, specifically triggering when the short-term window (2s) exceeds a long-term window (2m) by a set detection threshold. For all data streams, AUC was extracted by quantifying the area under the x-axis

for 1) 2s short-term window (short-term trend) ($2s - AUC(t) = \frac{\sum_{i=t-2}^{t+2} |iEEG(t)|}{2f}$, where f is sampling rate) and 2) a long-term window (long-term trend) (ambulatory: -60 to -2 s preceding magnet swiping to avoid swiping artifact/ in-lab: -90 to 0 s) (Figure 1B for ambulatory). Because the AUC detector works by the relative change in the short-term trend and the long-term trend, the power increase of the slow wave during sleep barely affects detection.

Peak analyses

For both ambulatory magnet swipe iEEG data, as well as the provocation task data, we extracted iEEG peaks as a secondary analysis to average AUC. We extracted and quantified peaks because peaks contribute most strongly to AUC averages, and we were interested in whether there were condition-dependent differences in number and size of peaks. The peaks were extracted using the MATLAB function to find local maxima (`findpeaks.m`). The following conditions to find peaks are decided heuristically based on given iEEG data: The minimum peak prominence was 25 μV , and the minimum peak to peak distance was 1 s.

We calculated the number of peaks per minute for each condition. We designated thresholds for relative changes in 5% intervals, and summed the number of peaks that exceeded that threshold for each interval (Figures 1E, 2C, and S2A). In Figures 1D, 2B, S2B, and S2C, sensitivity (the number of peaks exceeds the threshold divided by the total number of obsessive trials) and specificity (the number of peaks exceeds the threshold divided by the total number of neutral trials) were quantified for those peaks exceeding each threshold interval.

Power extraction and statistics

To better characterize the contributions of spectral power to the AUC estimates above, we performed time-frequency analysis using a multi-taper convolution method with discrete prolate spheroidal sequence tapers. The power was extracted by squaring the magnitude of the complex Fourier-spectra. The time window length was fixed to 1 s; the time step was 0.1 s and the frequency resolution was at 1 Hz. For provocation tasks with a pre-trial baseline, the power was transformed by the log function, and then spectrograms were subtracted by a 2-s baseline period. The statistical significance of between-condition comparisons was determined using a cluster-based permutation approach; the maximum sum of an independent-sample two-sided t test value with a significance level of 0.05, 1000 random permutations had been done (Figure 3B). The absolute power in both provocation tasks was extracted at the moment of 1s (Figure 3A, top: 1.0-1.1s; bottom: 0.9-1.0s). The null hypothesis (H_0) was the power of obsessive trials and the neutral trials were from the same distribution, and the alternative hypothesis (H_a) was the power in obsessive trials was higher than the neutral trials so one-sided Student's t test was performed. The significance level was indicated with FDR-adjusted $*p < 0.01$ (Figure 3C).

The Pearson correlation was estimated (Figure 1C) between the 2s-AUC short-term trend and the power estimates for each frequency ([1:1:120] Hz) for the ambulatory iEEG snapshots. We hypothesized the median of the correlation was zero in each frequency (H_0) to get the most significantly changed frequencies. The one-sample two-sided sign test was performed to get p values in each frequency, and FDR-adjusted $*p < 0.001$ was applied to reject the null hypothesis.

For ambulatory and detection data, we then extracted the spectral power at peaks below compared to exceeding 75% detection threshold (Figure 1F). For the ambulatory data, there were 11 peaks for obsessive snapshots (over 75%), and 222 peaks for both obsessive and control snapshots (below 75%). Significance was determined using one-sided Student's t test with 0.001 of significance level and assumed two variables were from normal distributions with unknown but equal variances (H_0).

rDBS programming

Bipolar stimulation for OCD was delivered to contacts 1(+) and 2(-) in the NAc and VeP respectively. The patient went home with the programmed settings at a charge density of 7.1 $\mu\text{C}/\text{cm}^2$, a current of 7.0 mA, a frequency of 125 Hz, a pulse-width-per-phase of 80 μs , and a burst duration of 1000 ms. Contacts 3(-) and 4(-) in the external globus pallidus (GPe) and Putamen from the NAc-VeP lead and contacts 3(+) and 4(+) in the temporal lobe from another lead delivered the stimulation for epilepsy.

We programmed 'detection-specific therapy' for this patient, which allows the first stimulation burst to be delivered for 1s only to the electrodes associated with the area where activity was detected. In other words, if a detection is made in the NAc-VeP, only the two electrode contacts flanking the NAc-VeP would deliver stimulation. If an unrelated detection is made in the right temporal lobe (e.g., for a seizure), only the temporal depth lead will receive stimulation. If the related detection is still captured after the stimulation, both related and unrelated contacts are stimulated simultaneously up to 4 more times (only possible after the initiation of OCD treatment, when the OCD electrodes were enabled). The number of following stimulations could not be reported because of the limitation of the device. The refractory interval for the stimulation is 1.28 s which means the following stimulation can't be delivered within 1.28 s after stimulation. The detection algorithm restarted when the refractory interval ends. During the stimulation, we could not analyze electrophysiology data because of the stimulation artifact.

Following a monopolar stimulation task to identify the appropriate stimulation settings, we activated rDBS for 24 h, and it was well-tolerated. We performed an acute stimulation task to define settings that induced improvement in mood, anxiety, and energy. Stimulation settings were set at 1 mA below the threshold for a mirth response. Further, we tested these settings with concurrent exposure to OCD triggers using similar procedures outlined in the "naturalistic provocation task".

rDBS therapeutic outcomes

Detections

rDBS detects above-threshold increases in AUC, and delivers stimulation in response. A single detection occurs when the increase in AUC between the short-term and long-term trend windows exceeds a programmed threshold. If rDBS detects above-threshold AUC increases more than five times following a stimulation delivery within a 20 s interval, called a long episode detection, 90 s of iEEG data are stored (30 s preceding the first detection, and 60 s following the first detection). The total detection count pools the number of detections across both single and long episode detections. The detection threshold was initially 75% (November 2019 to December 2020), and was increased to 87.5% beginning January 2021. The clinicians made this adjustment as an attempt to balance the

number of seizure and obsessive detection snapshots being recorded due to storage limitations of the NeuroPace device. The short-term window and the long-term window for the relative change in AUC were 2 s and 2 min respectively.

In [Figure 4B](#), we are quantifying the contribution of each power band to the AUC peak triggering a detection, over time. Specifically, for each peak and power band (delta: 1-4 Hz, theta: 5-8 Hz, alpha: 9-12 Hz, beta: 13-30 Hz, low gamma: 31-60 Hz, and high gamma: 61-120 Hz), we are looking at the power increase associated with the AUC increase underlying the peak. [Figure 4B](#) is designed to represent how we examined the “percent change” in low-frequency delta power for each peak relative to the other power bands. Relative changes in the power for each frequency band were calculated monthly from November 2019 to June 2022 (mean \pm SEM) ([Figure 4B](#)). Relative change is calculated for each detection as: 2s-AUC short-term trend / 90-s AUC long-term trend *100, summed across all 2-s AUC intervals in the detection snapshot, averaged over all detections captured in a given month.

Clinical

A clinician administered a Y-BOCS to the patient at baseline, as well as 24 h post NAc-VeP-rDBS activation, and again at 1 year 18 weeks. The patient provided Yale-Brown Obsessive-Compulsive Scale Self-Reported (Y-BOCS-SR) evaluations to assess OCD symptom severity 24 h post NAc-VeP-rDBS activation, and monthly following this. Logistically we were not able to clinically administer Y-BOCS at repeated intervals following baseline due to the timing of the COVID-19 pandemic, however Y-BOCS and Y-BOCS-SR have been found to be comparable.²² Y-BOCS-SR reports were the primary metric by which we measured the severity of the patient's OCD symptoms.^{20,21} The Y-BOCS and Y-BOCS-SR were visualized over 23 time points, from baseline to 2 years 22 weeks post-baseline.

Supplemental information

**Responsive deep brain stimulation
guided by ventral striatal electrophysiology
of obsession durably ameliorates compulsion**

Young-Hoon Nho, Camarin E. Rolle, Uros Topalovic, Rajat S. Shivacharan, Tricia N. Cunningham, Sonja Hiller, Daniel Batista, Austin Feng, Flint M. Espil, Ian H. Kratter, Mahendra T. Bhati, Marissa Kellogg, Ahmed M. Raslan, Nolan R. Williams, John Garnett, Bijan Pesaran, Desmond J. Oathes, Nanthia Suthana, Daniel A.N. Barbosa, and Casey H. Halpern

Supplemental Information

Responsive deep brain stimulation guided by ventral striatal electrophysiology of obsession durably ameliorates compulsion

Young-Hoon Nho*, Camarin E. Rolle*, Uros Topalovic, Rajat S. Shivacharan, Tricia N. Cunningham, Sonja Hiller, Daniel Batista, Austin Feng, Flint M. Espil, Ian H. Kratter, Mahendra T. Bhati, Marissa Kellogg, Ahmed M. Raslan, Nolan R. Williams, John Garnett, Bijan Pesaran, Desmond J. Oathes, Nanthia Suthana, Daniel A. N. Barbosa+, Casey H. Halpern+

Content:

Supplemental Figure 1, related to Figure 1

Supplemental Figure 2, related to Figure 2

Supplemental Figure 3, related to Figure 4

Supplemental Figure 4, related to Figure 4

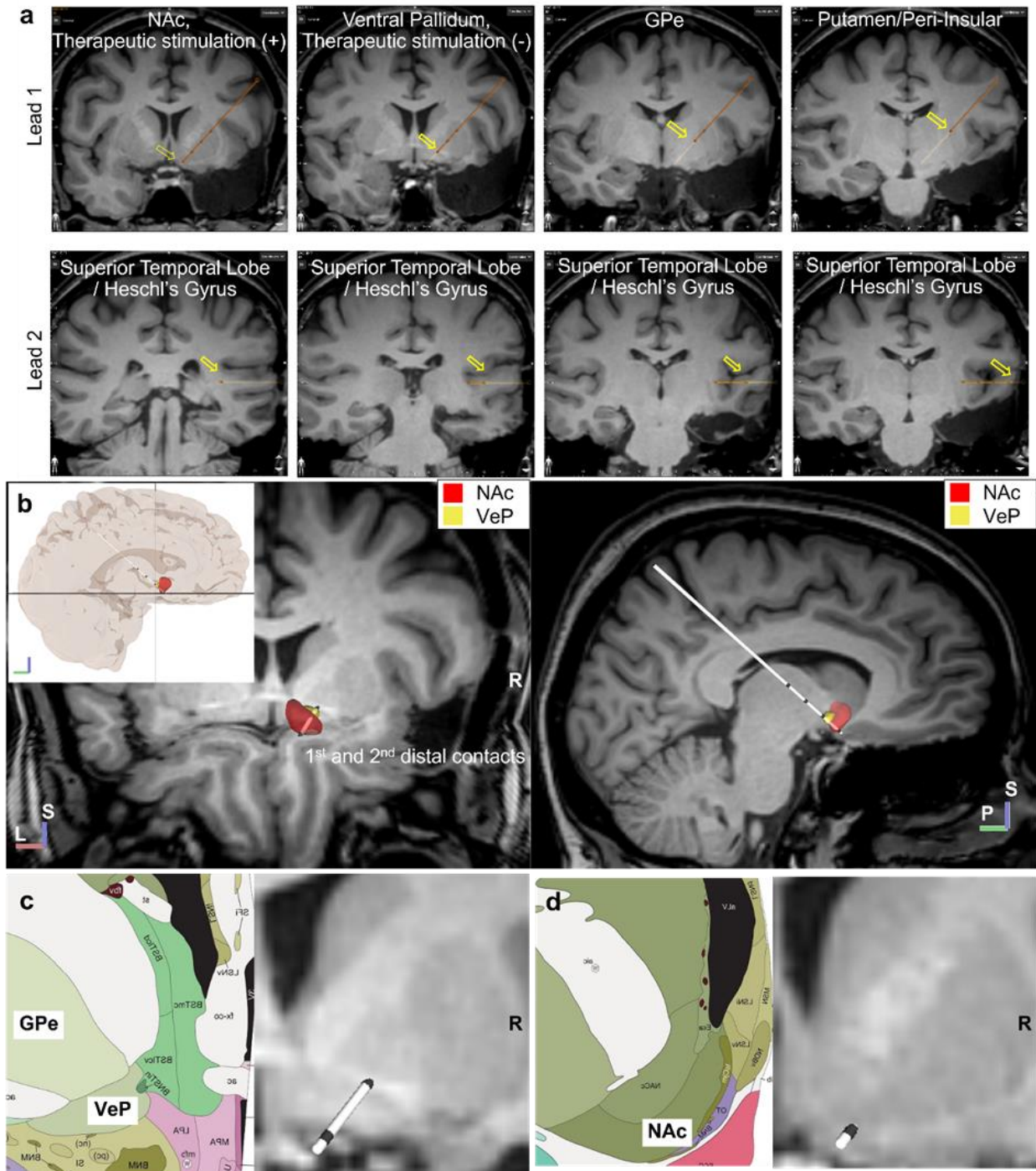


Figure S1. Treatment target, related to Figure 1. a, Two leads were placed ipsilaterally, one is targeting the right NAc for OCD (though traversing a predefined peri-insular seizure network more dorsally) and the other is targeting the right superior temporal lobe/Heschl's gyrus for epilepsy. The analysis in this paper is based on NAc-VeP bipolar re-referenced recordings. Therapeutic stimulation for OCD is delivered to NAc(+) and VeP(-). b, Coronal and sagittal planes of the brain with rDBS lead for OCD.

c, The coronal plane of the second distal contact with the brain atlas. The second distal contact was placed to the posterior border of the VeP. **d**, The coronal plane of the most distal contact. The first distal contact is in the NAc.

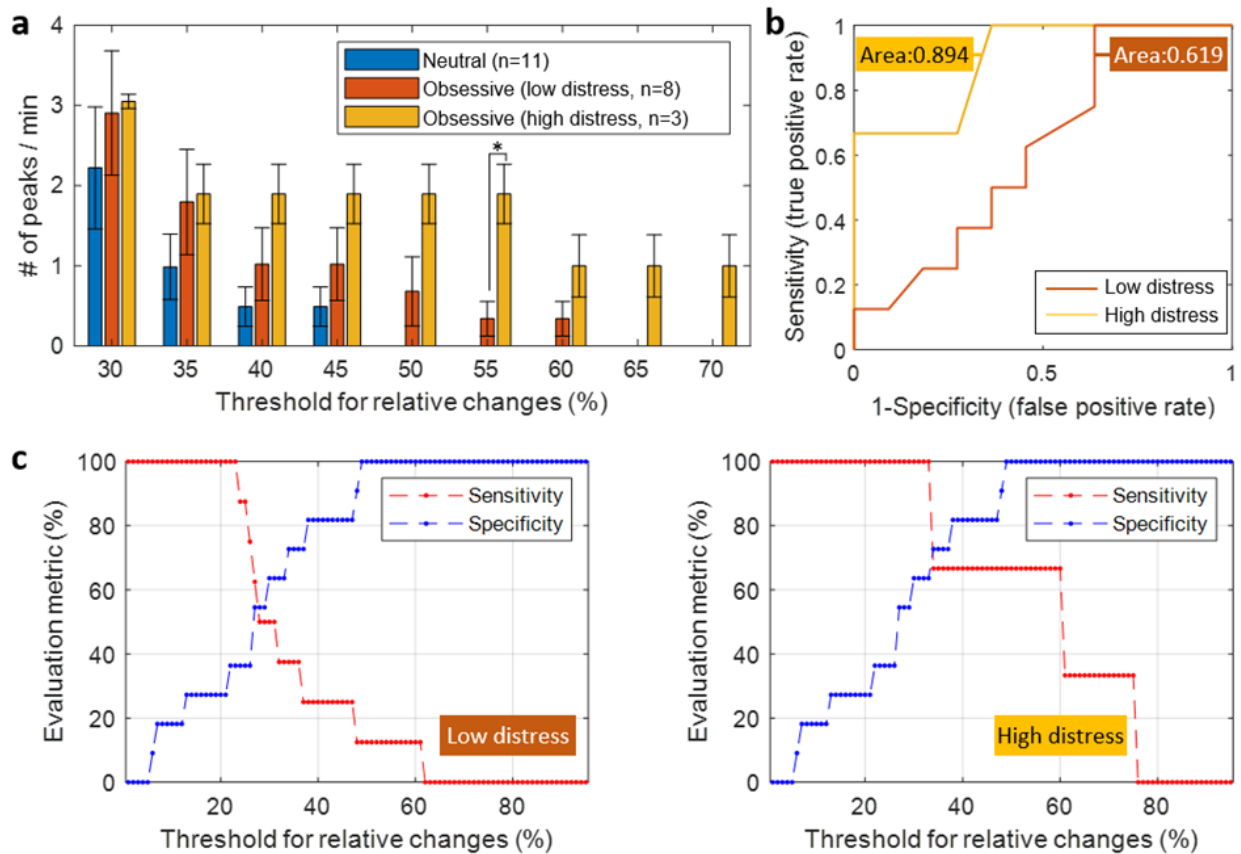


Figure S2. Dissociating high and low distress using VR-provocation, related to

Figure 2. a, The number of peaks extracted during relative changes in iEEG exceeding a range of thresholds per minute during the VR provocation task (mean±s.e.m.). The high distress trials are associated with higher relative AUC changes than the low distress. The number of peaks at -3 (high distress) was significantly higher than those of -2 (low distress) when a 55% threshold was applied ($*p=0.0386$, one-tailed t-test), but non-significant at other threshold levels. **b**, The area under the receiver operating characteristic (ROC) curve is 0.894 at the high distress ($n=3$). The area under the ROC curve is 0.619 at the low distress ($n=8$), suggesting the diagnostic accuracy (area under the ROC curve) was related to the obsession-related distress. **c**, Sensitivity and specificity trends from low distress (-2, left), and high distress (-3, right). This indicates that higher AUC peaks were observed in higher distress trials compared to lower distress trials, suggesting AUC peaks are greater with greater levels of distress.

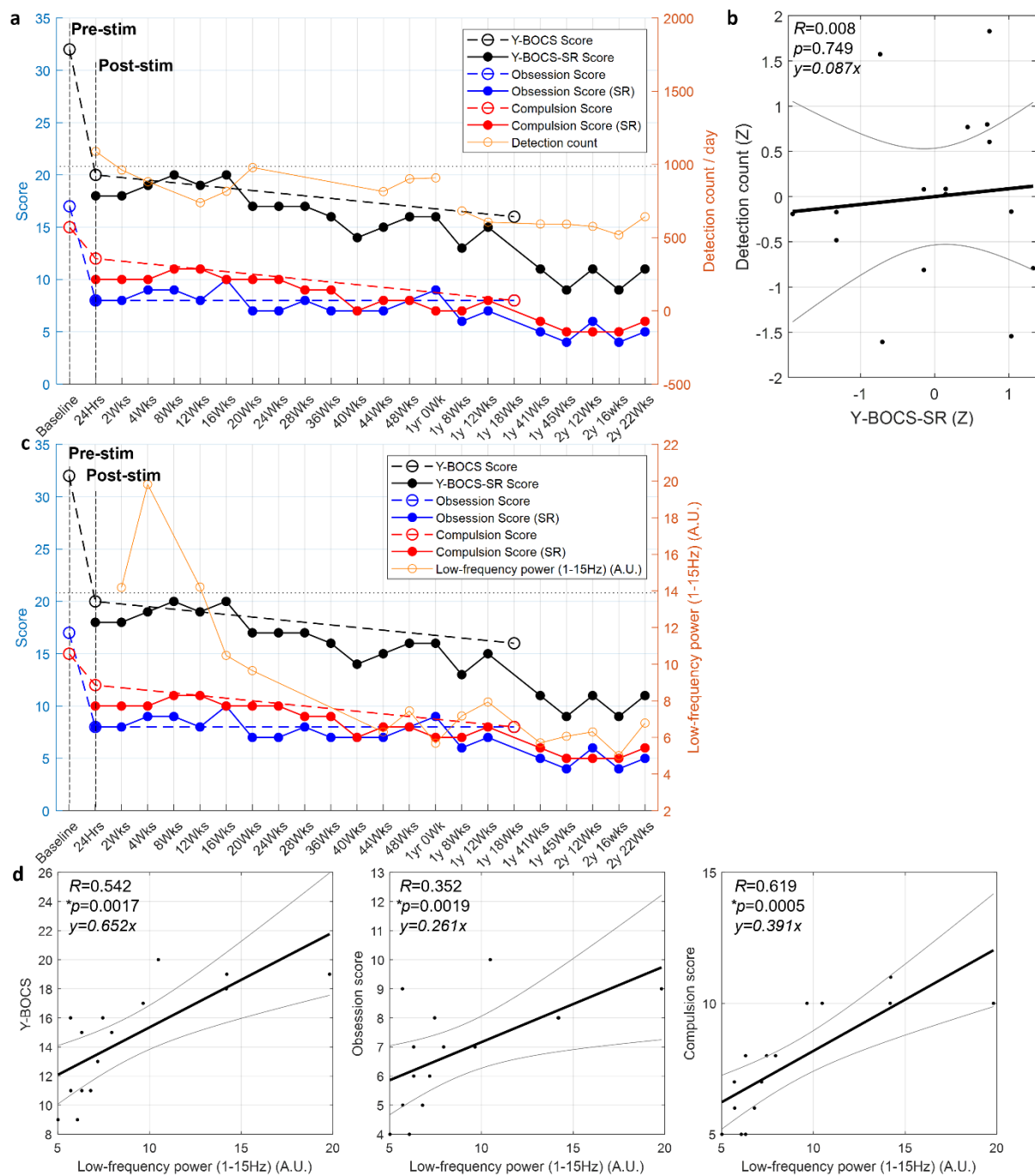


Figure S3. Detection count and average low-frequency power with Y-BOCS, related to Figure 4. a, Average detection count (the number of detection) over the 7-day period preceding when the patient reported Y-BOCS-SR was indicated by the orange line. There were 5 Y-BOCS datapoints (8, 24, 28, 36 and 40 weeks) that coincided in time with a rDBS device settings change (bandpass-based detector was also applied at these 5 time-points) so there was no detection count with the same setting. Correlations between the detection count and Y-BOCS-SR were analyzed. **b**,

Detection count did not correlate with Y-BOCS-SR ($p=0.749$). Detection count (orange) and Y-BOCS-SR (black) in **S3a** were divided into two groups before ($n=14$) and after ($n=7$) 2021 because the threshold was changed in January 2021. The detection count and Y-BOCS-SR were z-scored within the group, and the correlation for its pairs was calculated using linear regression ($n=21$). **c**, Average low-frequency power (1-15Hz) over the 7-day period preceding when the patient reported Y-BOCS-SR was indicated by the orange line. The low-frequency power was extracted from long episode iEEG data, and correlations between the detection count and Y-BOCS-SR were analyzed. To derive iEEG estimates corresponding in time with the Y-BOCS time-scale (self-reported symptoms over the last 7 days), each iEEG estimate used in the correlation was a 7-day average (yielding more than 40 iEEG snapshots). However, during the first 24-hours following stimulation being turned on, only 3 long episode detections occurred (resulting in the storage of only 3 iEEG snapshots), which was not enough data to sufficiently power a data-point to coincide with the 24-hours post-stim Y-BOCS (which captures the symptom severity of the preceding 7-days). Therefore, we were not able to generate an iEEG data-point for the 24-hour post-stim Y-BOCS. There were Y-BOCS datapoints (8, 24, 28, 36 and 40 weeks) that coincided in time with a rDBS device settings change (bandpass-based detector was also applied at these 5 time-points) so there was no long episode iEEG data with the same setting. **d**, Y-BOCS ($*p=0.0017$), Obsession score ($*p=0.0019$), and compulsion score ($*p=0.0005$) are significantly correlated with the low-frequency power (1-15Hz).

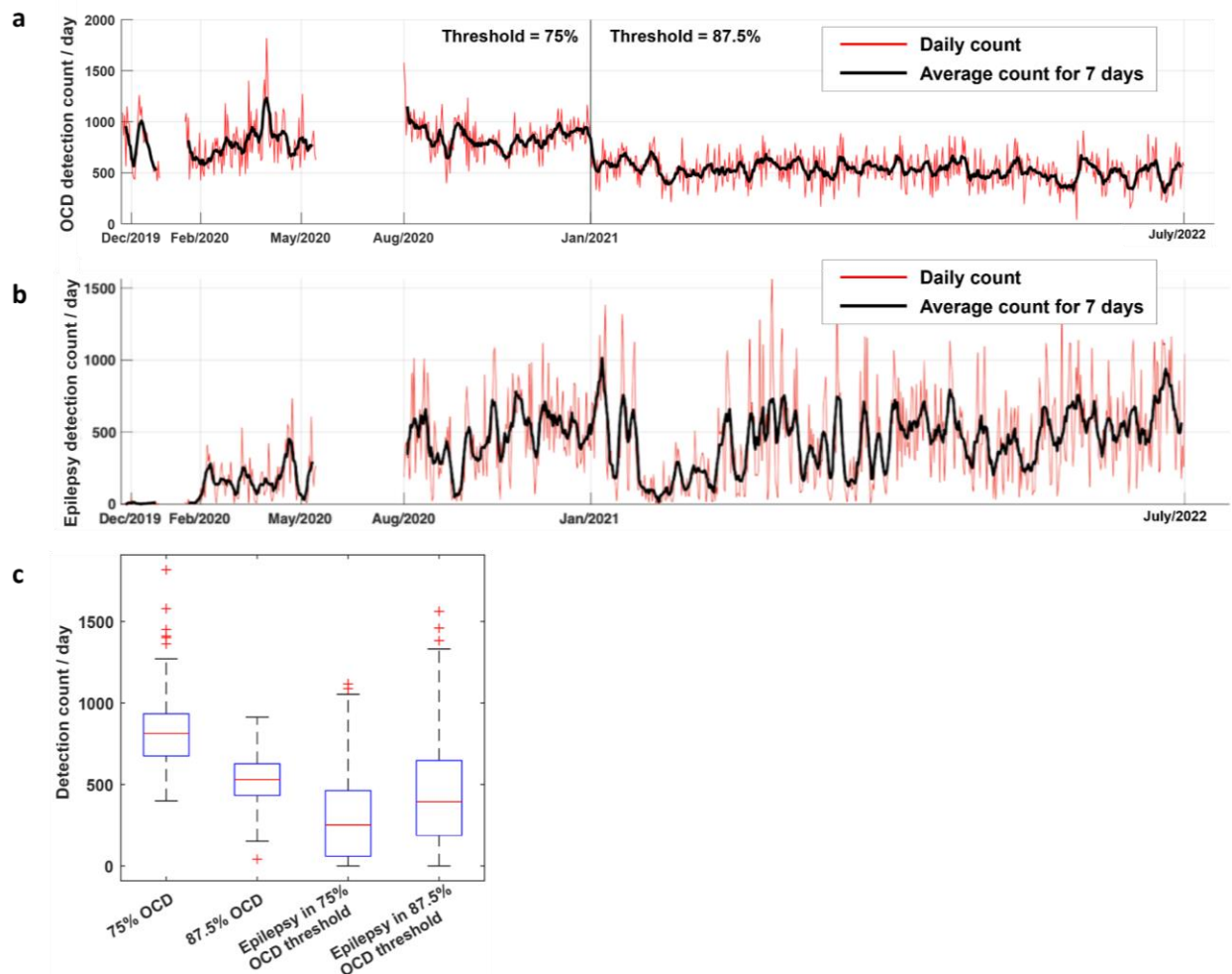


Figure S4. rDBS detection counts, related to Figure 4. a, The detection count (OCD) across time. Every rDBS detection results in a minimum of one stimulation (1s duration). **b,** The detection count (epilepsy) across the time. Double monopolar stimulation that likely modulated GPe (peri-insular target) was enabled from April/2019 (7 months before OCD stimulation onset). The current detection condition for epilepsy which is contacts 3(-) and 4(-) in the GPe and Putamen/Peri-Insular from the NAc-VeP lead and contacts 3(+) and 4(+) in the temporal lobe from another lead was applied from October/2019 (1 month before OCD stimulation onset). **c,** The median number of OCD detections (triggering stimulation) in the 75% threshold was 814/day, and that of 87.5% was 530/day. As the threshold of the detection was changed from 75% to 87.5% on Jan/2021, the number of detections at 87.5% threshold setting is significantly decreased from 75% threshold ($*p < 0.00001$, two-sample one-sided Wilcoxon rank sum test). The median number of the epilepsy detections was 251/day in the 75% threshold, significantly increased to 394/day in the 87.5% threshold ($*p < 0.00001$, two-sample one-sided Wilcoxon rank sum test). The patient had a ~60% reduction in epilepsy since the initiation of her epilepsy treatment, and this has remained stable.